Title:

Optimizing the evaluation of thermal transmittance with the thermometric method using multilayer perceptrons

Authors:

David Bienvenido-Huertas[1], Carlos Rubio-Bellido*[2], Juan Luis Pérez-Ordóñez[3], Juan Moyano[1]

[1]Department of Graphical Expression and Building Engineering, University of Seville, 41012 Seville, Spain; jbienvenido@us.es; jmoyano@us.es
[2]Department of Building Construction II, University of Seville, 41012 Seville, Spain; carlosrubio@us.es
[3]Department of Civil Engineering, University of A Coruña, E.T.S.I. Caminos, Canales y Puertos. Campus Elviña s/n, 15071 A Coruña, Spain; jlperez@udc.es

*Author to whom correspondence should be addressed;
Higher Technical School of Building Engineering, Ave. Reina Mercedes 4A, Seville, Spain
E-Mail: carlosrubio@us.es (C.R.B.); Tel.: +34-686-135-595

Highlights:

- Estimation of the values obtained with ISO 9869-1 by using the variables of the thermometric method.
- Determination coefficient greater than 98% in both approaches.
- Analysis of multilayer perceptrons designed for building periods.
- The methodology reduces the error associated with the thermometric method.

Abstract:

The characterization of building thermal behaviour is crucial to achieve the low-carbon objectives of the European Union by 2050. In this way, the knowledge of the thermal transmittance is being developed as a significant factor of the thermophysical properties of the envelope. In the existing building, the theoretical calculation has several limitations with non-destructive techniques typical of the deterioration of the elements. Many experimental methods obtain therefore more representative results. The experimental method developed in ISO 9869-1 is the most standardized, although it presents limitations in the heat flux measurement. However, the thermometric method obtains the thermal transmittance with the surface temperature. This research is focused on the evaluation of the thermal transmittance based on ISO 9869-1 (average method and average method with correction for storage effects), but using variables measured with the thermometric method. For this purpose, multilayer perceptrons were used as post-processing techniques. The models were trained by using a dataset of 22,820 simulated tests of representative walls of the building stock in Spain. The determination coefficient was greater than 98% in both analysis approaches. Individual models were also generated for each building period because they significantly influenced the input variables. The results showed that thermal transmittance values can be obtained without measuring the heat flux, and the error associated with the use of tabulated values for the total internal heat transfer can be removed. This research would guarantee a high assessment tax of buildings establishing adequate energy conservation measures to improve their energy performance.

Keywords:
Thermal transmittance; ISO 9869-1; thermometric method; multilayer perceptrons

Nomenclature

Symbols

C_k: thermal capacity of the layer k [J/(m2·K)]
F_{IN}: total internal thermal mass factor [J/(m2·K)]
$F_{IN,k}$: internal thermal mass factor for each layer k of the wall [J/(m2·K)]
F_{OUT}: total external thermal mass factor [J/(m2·K)]
$F_{OUT,k}$: external thermal mass factor for each layer k of the wall [J/(m2·K)]
MLP_{HL-1}: multilayer perceptron with 1 hidden layer
MLP_{HL-2}: multilayer perceptron with 2 hidden layers
MLP_{HL-3}: multilayer perceptron with 3 hidden layers
q_j: density of the heat flow rate per unit area at the instant j [W/m^2]
R: thermal resistance of the wall [(m2·K)/W]
$R_{IN,k}$: sum of the internal thermal resistances from the previous material to the indoor environment [(m2·K)/W]
R_k: thermal resistance of the layer k [(m2·K)/W]
$R_{OUT,k}$: sum of the external thermal resistances from the next material to the outdoor environment [(m2·K)/W]
$T_{IN,j}$: internal air temperature at the instant j [ºC]
$\overline{T}_{IN}$: mean of internal air temperature (input variable of multilayer perceptron) [ºC]

$T_{OUT,j}$: external air temperature at the instant j [ºC]
$\overline{T}_{OUT}$: mean of external air temperature (input variable of multilayer perceptron) [ºC]
$\overline{T}_{S-IN}$: mean of internal surface temperature (input variable of multilayer perceptron) [ºC]
U_{9869-1}: thermal transmittance obtained by the average method of ISO 9869-1
$U_{9869-1,Fk}$: thermal transmittance obtained by the average method with correction for storage effects of ISO 9869-1
$U_{MLP,\ 9869-1}$: estimated thermal transmittance by the multilayer perceptron (thermal transmittance obtained by the average method of ISO 9869-1)
$U_{MLP,9869-1,Fk}$: estimated thermal transmittance by the multilayer perceptron (thermal transmittance obtained by the average method with correction for storage effects of ISO 9869-1)
$w_{10}^{(2)}$: weight of the bias neuron of the hidden layer
$w_{lk}^{(2)}$: weights of the output layer
$w_{kj}^{(1)}$: weights of the hidden layer
x_j: values of the input layer
y_0: input value of the bias neuron of the hidden layer
$\hat{Y}_{MLP}$: value estimated by the multilayer perceptron

Greek symbols
Δt: time interval between two readings [s]
δT_{IN}: difference between the average internal air temperature from the 24 h before measuring the observation and the average internal air temperate from the first 24 h of the test [ºC]
$\overline{\delta T}_{IN}$: mean of δT_{IN} (input variable of multilayer perceptron) [ºC]
δT_{OUT}: difference between the average external air temperature from the 24 h before measuring the observation and the average external air temperature from the first 24 h of the test [ºC]
$\overline{\delta T}_{OUT}$: mean of δT_{OUT} (input variable of multilayer perceptron) [ºC]
σ: activation function

Abbreviations
BFGS: Broyden-Fletcher-Goldfarb-Shanno algorithm
ECM: Energy Conservation Measure
FEM: Finite Element Method
GHG: Greenhouse Gases
MAE: mean absolute error
MLP: multilayer perceptron
P1: building period anterior to NBE-CT-79
P2: building period between NBE-CT-79 and CTE
P3: building period posterior to CTE
R^2: coefficient of determination
RMSE: root mean square error
U: thermal transmittance

1. Introduction

The deceleration of climate change and the decrease of environmental degradation are the main challenges of society [1]. Such situation, among others, is more and more extreme because of the high energy consumption. Particularly, the building stock seriously affect such energy consumption. In quantified data, buildings are responsible for 40% of the total energy consumption in the European Union [2,3]. Concerning the residential buildings, the percentage of contribution in the energy consumption is 24.79%. Buildings are also responsible for 36% of the Greenhouse Gases (GHG) emitted to the atmosphere [4,5], thus highlighting the deficient energy performance of the existing buildings. Other issues with a higher incidence in recent years, such as the energy poverty [6,7] and the increase of the mortality percentage in winter and summer because of not having acceptable thermal comfort conditions [8,9], are raising the awareness of the need for improving the energy performance of buildings through international guidelines and objectives. The European Union has established a roadmap for moving to a low carbon economy by 2050 [10]. The goal is to reach an economy which practically does not emit GHF to the atmosphere. As for the building sector, the objective is to reduce GHG emissions by 90% with respect to the levels in 1990 [10].

To reach such objective, the energy performance of buildings should be improved. In this way, the energy consumption of residential buildings is the sum of the consumption associated with different usages, such as the use of equipment and lighting systems. Nevertheless, the use of air conditioning systems is among the highest consumption sources [11,12]. The implementation of energy conservation measures (ECMs) reducing such consumption would therefore mean an important decrease of GHG emissions.

For this purpose, characterizing the thermal behaviour of buildings is fundamental to establish effective ECMs [13,14]. The envelope elements play an important role in the thermal behaviour of buildings (due to the heat losses or gains [15,16]), with façades being the most influence envelope elements because they are the greatest surface area in contact with the exterior [17]. Among their various thermophysical properties, the thermal transmittance is one of the most important [18–

20] because it varies heat losses and influences the energy demand [21,22]. A correct determination of the thermal transmittance will therefore contribute to select effective ECMs as well as to reduce the payback periods [23].

Thermal transmittance can be determined through theoretical calculations or non-destructive experimental methods [24]. The theoretical calculation method is developed in ISO 6946 [25]. The calculation is made by considering both the thermal resistance of each layer composing the wall and its contributions of internal and external surface thermal resistance (for walls, the internal surface thermal resistance is 0.13 m^2K/W and the external is 0.04 m^2K/W). Although it is a method widely used by professionals and state standards, a high level of uncertainty is presented in the estimations of thermal transmittance [21], since the accurate typology of layers, thicknesses, and thermal conductivity values are in most cases unknown [26]. Therefore, the technique used to estimate the composition of the wall significantly influences the whole calculation procedure. There are three typologies for determining the composition of a wall: (i) estimation by analogous constructions and visual inspection [27,28]; (ii) use of technical documentation of the building [29]; and (iii) endoscopic analysis [30]. Among such techniques, the first technique has the highest associated uncertainty, whereas the second and third are the most effective options [26]. However, the lack of documentation of many buildings and the havocs generated by the endoscopies make their use something of a challenge [21]. Also, the use of the ISO 6946 method can be limited by other aspects, such as the presence of moisture [31], the ageing of materials [32], or the variation of the thermal conductivity by environmental conditions [33]. For this reason, the experimental methods are an opportunity to obtain more representative results. A total of 3 methods with different characteristics can be distinguished: the method included in ISO 9869-1 [34] (also known as the heat flow meter method), the infrared thermography methods [35,36], and the thermometric method [29,37,38].

The method in ISO 9869-1 is the only one being developed in a standard. Measuring the heat flux of the wall and the internal and external air temperatures is required to determine the thermal transmittance. Such method is widely used, but there is a series of operational requirements limiting the obtaining of representative results. Many limitations are associated with the heat flux measurement [39]. In this sense, Trethowen [40], Desogus et al. [41] and Cesaratto et al. [42] highlighted the disturbance generated by the location of the heat flux plate in the heat flux of the wall. In addition, the heat flux plate in the wall can influence the results obtained [43]. According to this, Meng et al. [44] established that the error in the evaluation of the thermal transmittance can reach 26% because of placing the plate. Moreover, other possible factors affecting monitorings have been indicated by many research studies. The most important is the need for using a high thermal gradient when performing tests. Desogus et al. [41] concluded that thermal gradients of 10 ºC obtain low uncertainties, which can be even more reduced as the thermal gradient increases. Given the difficulties to achieve high thermal gradients, a common practice is the use of HVAC systems. However, the effect of the operational cycles of HVAC systems should be also considered in data analysis [45] because the heat flux of the element generally increases when the heating equipment is activated. The data post-processing by removing such increases of heat flux could imply the obtaining of more representative results [45].

The presence of water in the wall (e.g., because of interstitial condensations) also can affect the results because of the higher thermal conductivity of the wall [31]. Condensations can therefore mean variations of up to 71% in the thermal transmittance measured with respect to that obtained under normal conditions [31,46]. Pipes inside the wall with temperatures different to the wall temperatures also affect the representation of results [47]. The orientation of the wall is another factor to be controlled. Ahmad et al. [48] showed that walls facing north have a greater stability in the heat flux, whereas deviations greater than 37.3% can be reached in other orientations (e.g., west, east, and south). Finally, the minimum test duration depends on both the theoretical thermal transmittance is thought that the wall has and the variability of the environmental conditions [49], reaching durations ranging from 1 night (for light walls), 3 days, and even 1 week [21].

Some research studies have therefore analysed the possibilities of applying the heat flow meter method : (i) Lucchi [50] evaluated 14 historical brick walls with the method developed in ISO 9869-1. The results showed deviations between the measured and calculated values according to the Italian standard, thereby reflecting the possible overestimation performed by theoretical procedures, particularly in old buildings; (ii) in a later study, Lucchi [51] conducted an experimental campaign using a sample of 10 historical stone walls. The results showed again deviations between the measured values and that obtained by tabulated procedures; (iii) such overestimation performed by the tabulated values with respect to the measured values with ISO 9869-1 was also reflected by Rotilio et al. [52]. In this study, the authors monitored 4 masonry walls. The results reflected deviations between 10 and 15% between the measured and the established value by the standard of the area. Also, the authors found limitations to carry out tests in damaged walls (e.g., because of earthquakes); (iv) Gaspar et al. [53] analysed the performance of the method included in ISO 9869-1 in a wall with a high thermal resistance (the theoretical thermal transmittance was 0.27 $W/(m^2K)$). Given the low heat flux that can be measured, the deviation in the estimation of thermal transmittance was reduced by 1.9% in a monitoring of 72 h by using a thermal gradient of 19 ºC. The test duration was increased for lower temperature differences; (v) Asdrubali et al. [54] analysed 6 walls designed by following principles of bio-architecture. The results showed deviations with reference values between 4 and 75%, possibly due to factors such as the overestimation of the thermal conductivity values or the environmental factors during the test; and (vi) Ficco et al. [26] analysed the effectiveness of the method in 7 vertical envelope components of various materials (including a double glass with air gap) by using 3 different plates. The results obtained an acceptable degree of adjustment in all cases and in the 3 plates used. The method described in ISO 9869-1 obtained therefore representative results despite the possible limitations associated with such method because of the heat flux plate and environmental aspects.

Given the difficulties of measuring the heat flux, the infrared thermography has arisen in recent years as an alternative for the method in ISO 9869-1 through various approaches. Such approaches are addressed to measure the surface

temperature of the wall and determine the variables of radiation transfer, such as the emissivity or the reflected apparent temperature [55]. The main difference among methods is because of both the location of the camera during the monitoring and the term used for the convective coefficient. Methods from the exterior [56] and the interior [57] can be therefore distinguished. The main advantage of such methods is that the tests can be performed in short periods of time [58] if the ideal test conditions are met (e.g., a thermal gradient between 7 and 16 ºC [59]). In addition, the thermal heterogeneities presented by the wall can be evaluated by using the infrared camera [60].

A similar approach is found in the thermometric method. Such method consists of determining the thermal transmittance of a wall by measuring its surface temperature and the internal and external air temperatures [29]. Neither the heat flux (as in the heat flow meter method) nor variables of the radiation component (as in infrared thermography methods) are required to be measured, thereby simplifying the calculation process. Given the heat flux is not required to be measured, errors of up to 26% because of placing the plate, which are indicated by Meng et al. [44], are not produced in this method. In such study [44], the authors reflected that the error in the evaluation of the thermal transmittance by measuring surface temperature is reduced by 6% (i.e., the error is reduced by 20%). Apart from this, the thermometric method has similarities in the operational requirements established by the heat flow meter method. In this way, a high thermal gradient, test duration, orientations, etc., which have been indicated above for the heat flow meter method, are also required by the thermometric method [29,37]. In addition, analysis procedures have been adapted by some studies [61,62] with the aim of using the method widely.

One of the main aspects limiting the method is the value used for the total heat transfer coefficient. In this sense, most applications of the method have used tabulated value for the internal total heat transfer coefficient from ISO 6946 (7.69 $W/(m^2K)$). Some research studies have stressed the accuracy of the results obtained with the method by using such value: (i) Bienvenido-Huertas et al. [29] analysed the application of the method in 8 case studies. The results obtained deviations lower than 20% between the reference and the measured values in 6 of the case studies; (iii) Kim et al. [37] applied the thermometric and the heat flow meter methods in 4 walls before and after improvement performances. The deviations ranged between 0.13% and 6.74% in the 8 tests; and (iii) later, Kim et al. [38] analysed the influence of the internal total heat transfer coefficient. The tabulated values from both ISO 6946 and Korea Energy Savings Design Standard were used, and then compared with the results obtained by the heat flow meter method. The results determined that the value from ISO 6946 obtained the best results, with error percentages lower than 8.6% with respect to the heat flow meter method.

Nevertheless, deviations can occur when the tabulated values are used to characterize the thermal transmittance. Evangelisti et al. [63] found deviations of up to 37% between the heat fluxes obtained with tabulated values and those measured in situ. Such deviations could be caused by using HVAC systems. Bienvenido-Huertas et al. [57] also found limitations in the use of the tabulated value from ISO 6946 when obtaining accurate estimations of thermal transmittance by using infrared thermography methods.

To avoid possible deviations between the heat flow meter method and the thermometric method (because of using tabulated values in the latter), this research suggests a new approach by using artificial neural networks. Thermal transmittance was therefore evaluated according to the approaches included in ISO 9869-1, but using the variables measured by the thermometric method. For this purpose, the design of a model used in a previous research [62] to evaluate the heat storage corrections is optimized. It is important to stress that the advantages of using data analysis techniques by means of artificial intelligence for the thermal characterization of several components have been reflected in various research works: (i) Buratti et al. [64] developed an artificial neural network to estimate the thermal transmittance of wooden windows by using parameters easily to be determined (e.g., type of window or framework thickness); (ii) Chudzik [65] used artificial neural networks to predict the heat transfer coefficient in the surface of insulating material, thus determining their thermal properties; and (iii) Aznar et al. [66] used feed-forward time-delay neural networks to estimate the temperature value predicted in the following 30 minutes in each layer composing the wall. The use of such data analysis techniques constitutes therefore an opportunity to make accurate estimations.

To achieve the objectives proposed in this study, various prediction models were generated to predict the two analysis typologies set by ISO 9869-1. The models were trained by using a dataset of 22,820 simulated tests of representative walls of the building stock in Spain. The novelty of this study is, on the one hand, the optimization of the performance obtained in the methodological approach carried out in a previous research [62] and, on the other hand, the establishment of an analysis methodology allowing the results of ISO 9869-1 to be obtained by following the principles of the thermometric method (i.e., to measure the surface temperature instead of the heat flux). Likewise, such methodology allows the correction procedure for storage effects of ISO 9869-1 to be applied without the need of knowing the layers of the wall. The results of this research aims at providing an analysis technique for auditors and engineers to carry out high audit taxes in buildings (by reducing the economic limitations of acquiring the equipment from ISO 9869-1 and guaranteeing the representation of the results), thereby easing the achievement of the objectives proposed by the European Union for 2050 [10].

This paper is structured as follows: after the introduction, Section 2 describes the methodology used. For this purpose, the calculation methods analysed, the characteristics of the multilayer perceptrons developed, the dataset used, and the training and testing procedures are described; Section 3 shows and discusses the results; and Section 4 provides the main conclusions.

2. Methodology

2.1. Calculation methods analysed

The most used method to characterize the thermal transmittance is the average method from ISO 9869-1 [21]. Such method considers that the oscillations can be damped by the average of the instantaneous heat flux measurements and the differences of internal and external air temperature in an increasing period of time, leading to a thermal transmittance value at steady state. The thermal transmittance is obtained by dividing the sum of the heat flux by the sum of the temperature differences of internal and external air (see Eq. (1)).

$$U_{9869-1} = \frac{\sum_{j=1}^{n} q_j}{\sum_{j=1}^{n} (T_{IN,j} - T_{OUT,j})} \quad (1)$$

Where q_j [W/m²] is the density of the heat flow rate per unit area at the instant j, and $T_{IN,j}$ and $T_{OUT,j}$ [K] are the internal and external ambient temperatures at the instant j.

The ISO 9869-1 standard itself suggests a modification of Eq. (1) considering the heat storage effect [34]. The standard indicates that such modification should be used when the value obtained at the end of the test varies more than 5% with respect to that measured 24 h before or to that in the first period, obtained as INT($2xD_T/3$), where INT is the whole part and D_T is the total days of test duration [34]. The procedure consists of modifying the heat flux through the wall according to the capacities of heat storage of its layers. Knowing previously the wall is required to be used, so it can be limited. Also, knowing the thermal properties of layers composing the wall is required.

For each layer k of the wall, the external and internal thermal resistance is calculated, thus obtaining the respective internal (Eq. (2)) and external (Eq. (3)) thermal mass factor. The sum of such factors obtains the total internal (Eq. (4)) and external (Eq. (5)) thermal mass factor.

$$F_{IN,k} = C_k \left[\frac{R_{OUT,k}}{R} + \frac{{R_k}^2}{3R^2} - \frac{R_{IN,k} R_{OUT,k}}{R^2} \right] \quad (2)$$

$$F_{OUT,k} = C_k \left[\frac{R_k}{R} \left\{ \frac{1}{6} + \frac{R_{IN,k} + R_{OUT,k}}{3R} \right\} + \frac{R_{IN,k} R_{OUT,k}}{R^2} \right] \quad (3)$$

$$F_{IN} = \sum_{k=1}^{N} F_{IN,k} \quad (4)$$

$$F_{OUT} = \sum_{k=1}^{N} F_{OUT,k} \quad (5)$$

Where $F_{IN,k}$ [J/(m²·K)] is the internal thermal mass factor of the layer k, C_k [J/(m²·K)] is the thermal capacity of the layer k, $R_{OUT,k}$ [(m²·K)/W] is the sum of the outside thermal resistances from the next material to the outdoor environment, R [(m²·K)/W] is the thermal resistance of the wall, R_k [(m²·K)/W] is the thermal resistance of the layer k, $R_{IN,k}$ [(m²·K)/W] is the sum of the inside thermal resistances from the previous material to the indoor environment, $F_{OUT,k}$ [J/(m²·K)] is the external thermal mass factor of the layer k, F_{IN} [J/(m²·K)] is the total internal thermal mass factor, and F_{OUT} [J/(m²·K)] is the total external thermal mass factor.

To apply the correction, the numerator of Eq. (1) should be replaced with the expression of Eq. (6), finally obtaining the equation of the procedure with correction for storage effects (Eq. (7)).

$$\sum_{j=1}^{n} q_j - \frac{(F_{IN} \delta T_{IN} + F_{OUT} \delta T_{OUT})}{\Delta t} \quad (6)$$

$$U_{9869-1,Fk} = \frac{\sum_{j=1}^{n} q_j - \frac{(F_{IN} \delta T_{IN} + F_{OUT} \delta T_{OUT})}{\Delta t}}{\sum_{j=1}^{n} (T_{IN,j} - T_{OUT,j})} \quad (7)$$

Where δT_{IN} [K] is the difference between the average internal air temperature of the 24 h before measuring the observation and the average internal air temperature of the first 24 h of the test, δT_{OUT} [K] is the difference between the average external air temperature of the 24 h before measuring the observation and the average external air temperature of the first 24 h of the test, and Δt [s] is the time interval between two readings.

In general terms, the use of the two approaches proposed by ISO 9869-1 obtain very similar results [32,67], although the heat storage effect reduce the test duration. In particular, Deconinck et al. [67] highlighted that a deviation percentage of 10% was obtained by the average method 8 days after starting the test, whereas such percentage was obtained by the

average method with correction for storage effects at the 3rd day. Choi and Ko [32] also determined that the standard deviation of the average method was 0.160 at the 5th day, whereas for the method with correction was from 0.036 at the 2nd day to 0.006 at the 4th day. So, both the deviation and the test duration were reduced with the correction procedure.

The two approaches suggested by the standard are therefore effective data analysis techniques to be used. Nevertheless, knowing the number and characteristics of the layers in a wall limit the practical use of the approach with storage correction. Among the various techniques allowing the composition of a wall to be known, only the use of reliable technical documentation [27] or the endoscopy [30] are effective. However, the lack of documentation or the havocs generated by the endoscopies mean that such techniques are not used in most audits [27], so the use of the correction method from ISO 9869-1 is very limited.

2.2. Multilayer perceptrons

In a previous study [62], the authors of this paper analysed the use of multilayer perceptrons to estimate the correction procedure adapted to the thermometric method. The thermal transmittance value was determined by applying heat storage corrections to the heat flux obtained with the approach of the thermometric method (i.e., the heat flux is obtained by using the Newton's Law of Cooling and considering that the total heat transfer coefficient is 7.69 W/(m^{2}K)). The result obtained was not therefore determined according to the heat flux measurements. The novelty of such approach was the determination of heat storage corrections without knowing the layers of the wall. This aspect was achieved by using multilayer perceptrons (MLPs).

The MLPs are one of the typologies of artificial neural networks providing the best features because of their capacities of universal approximation [68–70]. It is a mathematical model inspired by the brain structure to solve different non-linear problems [71]. It is therefore an effective technique to solve regression [72] and classification [73] problems.

The architecture of the MLPs is made up of three kind of layers: an input layer, one or several hidden layers, and one output layer. There is a series of nodes (also known as neurons) connected among them in each layer. The estimation given by the MLP corresponds with the output value of the node of the last layer. Such value is the sum of the values of nodes of the previous layers weighted by synaptic weights and using activation, transfer, and propagation functions. The output value ($\hat{Y}_{MLP}$) can be therefore expressed by using the following equation to consider 1 hidden layer:

$$\hat{Y}_{MLP} = w_{10}^{(2)} y_0 + \sigma\left(\sum_{k=1}^{M} w_{lk}^{(2)} \sigma\left(\sum_{j=0}^{d} w_{kj}^{(1)} x_j\right)\right) \quad (8)$$

Where $w_{10}^{(2)}$ and y_0 are the weight and the value of the bias neuron of the hidden layer, $w_{lk}^{(2)}$ are the weights of the output layer, σ is the activation function, $w_{kj}^{(1)}$ are the weights of the hidden layer, and x_j are the values of the input layer.

In this research, the same approach of typologies of input variables was used as in the previous study [62]. So, T_{in}, T_{out}, $T_{s,in}$, δT_{in}, δT_{out}, the thickness, the building period, and time were considered as input variables. However, several aspects were modified with respect to the previous approach. Firstly, the data vector obtained at the end of the test was used to avoid reproducing the estimation of thermal transmittance through the whole time serie. For this purpose, average values for the temperature variables and the total test duration were used to modify the input variables, thereby reducing the complexity of applying the method and increasing the performance in the estimations. Given two calculation procedures used by ISO 9869-1 are described in Section 2.1, two different approaches were used to design the MLPs according to the output variable. Both MLPs estimating the thermal transmittance obtained by the average method and MLPs estimating the thermal transmittance obtained by the average method with heat storage corrections were developed. Table 1 indicates the input and output variables considered in this paper. Concerning the variable of the building period, it is worth highlighting that three values were considered to group the most representative building periods of the study area. As indicated in Section 1, the field of study of this research was the constructive typologies of the walls of buildings built in Spain. Three representative building periods in Spain can be highlighted, grouping the buildings of the zone [74,75]: P1 (anterior to the normative NBE-CT-79 [76]); P2 (posterior to NBE-CT-79 and anterior to the Spanish Technical Building Code [77]); and P3 (posterior to the Spanish Technical Building Code). The existing differences between such building periods are quite important because the envelopes built anterior to NBE-CT-79 are characterized by no having insulation as well as by being made up of one or several layers where the main element is the brick [78]. On the other hand, the consecutive implementation of NBE-CT-79 and then the Spanish Technical Building Code has led to design walls with more and more greater thicknesses of insulating material [79].

Table 1. Input and output variables used in each approach.

Approach	Input variables	Output variables
Approach 1	$\overline{T}_{IN}$, $\overline{T}_{OUT}$, $\overline{T}_{S-IN}$, $\overline{\delta T}_{IN}$,$\overline{\delta T}_{OUT}$, thickness, building period, time	$U_{MLP,\ 9869-1}$ [a]
Approach 2	$\overline{T}_{IN}$, $\overline{T}_{OUT}$, $\overline{T}_{S-IN}$, $\overline{\delta T}_{IN}$,$\overline{\delta T}_{OUT}$, thickness, building period, time	$U_{MLP,9869-1,Fk}$ [b]

[a] The thermal transmittance obtained by the average method of ISO 9869-1; [b] Thermal transmittance obtained by the average method with correction for storage effect of ISO 9869-1.

In addition, various architectures of the MLPs were analysed in this paper by varying the number of hidden layers in different models (Figure 1). In particular, architectures of 1 hidden layer (MLP_{HL-1}), 2 hidden layers (MLP_{HL-2}), and 3 hidden layers (MLP_{HL-3}) were analysed. A total of 3 different models were therefore developed for each approach according to the architecture used. The optimal number of nodes was also determined for each type of architecture. For this purpose, numbers oscillating between 2 and 15 nodes were analysed in each hidden layer.

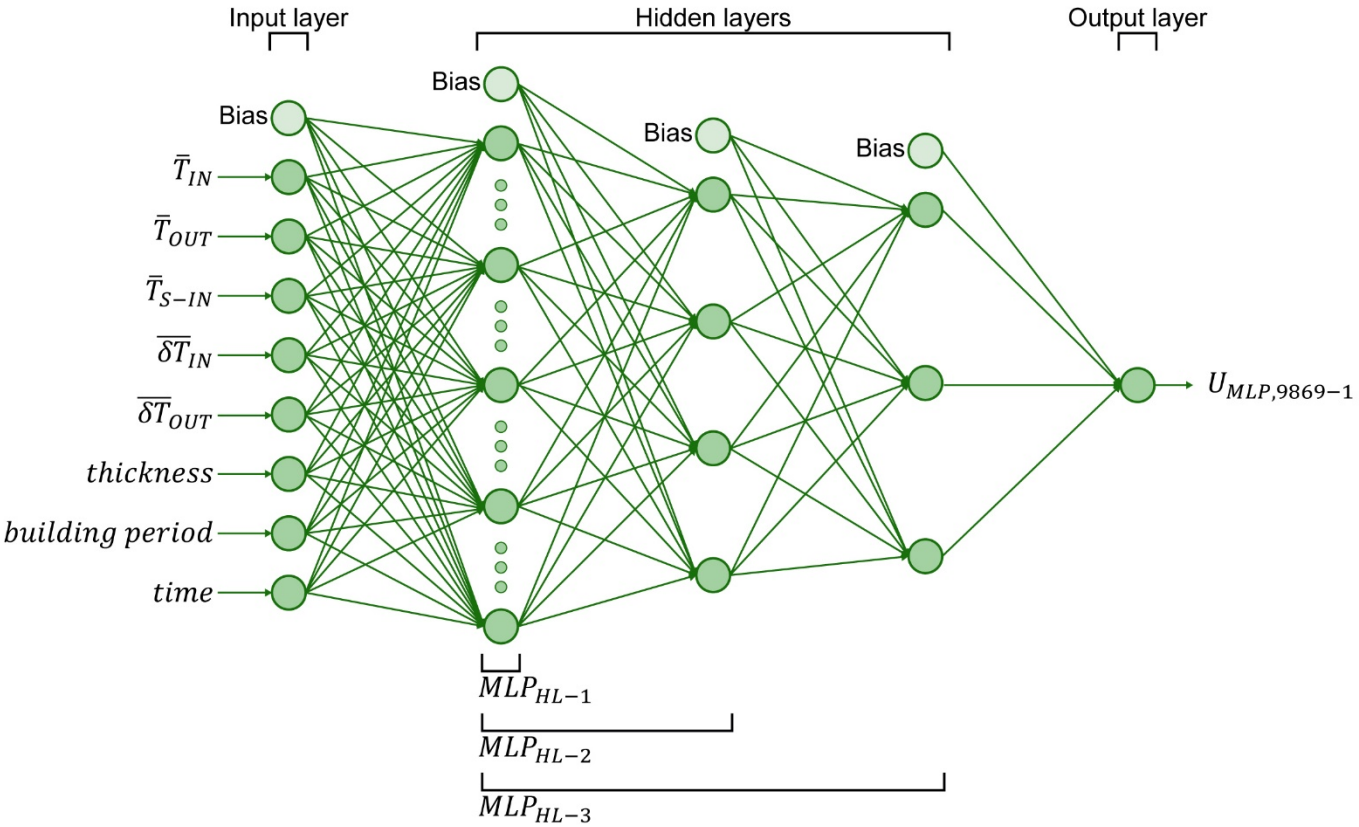

Figure 1. Scheme of the architectures considered for the MLPs of approach 1.

In this research, the MLPs were trained with backpropagation [80–82], using the Broyden-Fletcher-Goldfarb-Shanno (BFGS) [83] algorithm. Also, a 10-fold cross validation was used in the training of the MLPs. The cross validation allows the bias and the variance of the model to be reduced [84]. The 10-fold cross validation consists of randomly dividing the training dataset into 10 subsets. For each fold, 9 subsets were used for the training of the MLP, and the remaining subset was used for the testing. This process was repeated in the 10 folds. The performance of the MLP was obtained by the average value of the 10 folds. The dataset used for the training and testing is described in Section 2.3.

2.3. Dataset, training, and testing

To generate the dataset used for the training and testing of the models, a high test sample was intended to be used. Data from 69 tests were used in the previous research. Given the considerable time for performing a big sample of tests, two-dimensional transitory simulations were conducted by using Finite Element Methods (FEM). For this purpose, 140 typologies of walls were modelled. Such walls were representative of the building stock in Spain. Different sources, such as the Constructive Elements Catalogue [85] or those from several studies [78,86] were used. These walls belong to the 3 building periods of the zone to be studied and described in Section 2.2. Each model was simulated by using time series from monitorings carried out in real case studies (i.e., using actual measurements of internal and external air temperature). A total of 163 different monitoring data were used. The combination of the modelled walls with the time series generated therefore a total of 22,820 tests. The data acquisition interval was 15 min because it is used in other studies [29,62] and hastens the process of simulation. Given that the proposed methodology uses the average values obtained at the end of the test, each test contributed to the dataset with an observation (i.e., the dataset used was composed by 22,820 observations). Heat flux and surface temperature were measured at a distance of 1.50 m from the junction of the wall with the floor to avoid the influence of thermal bridges. It is worth stressing that the monitorings used were performed in different seasons of the year (Figure 2) with the aim of applying the estimations carried out by the MLPs to measurements conducted in any season. In addition, such time series were made with various thermal gradient so that the MLPs could perform accurate estimations, both under favourable and unfavourable test conditions. The test duration was also different to provide greater variability to the observations included in the dataset. A total of 163 time series of external and internal air temperature obtained by monitoring walls were used and both surface temperature and heat flux values were recorded, so such monitorings were used to validate the simulations. Deviations between actual and simulated values were analysed. The mean error obtained

was less than 10% after removing data from the first 12 hours of the simulation because such data could increase the error up to 20%. Thus, the representation of the variables of surface temperature and heat flux obtained from simulations was guaranteed.

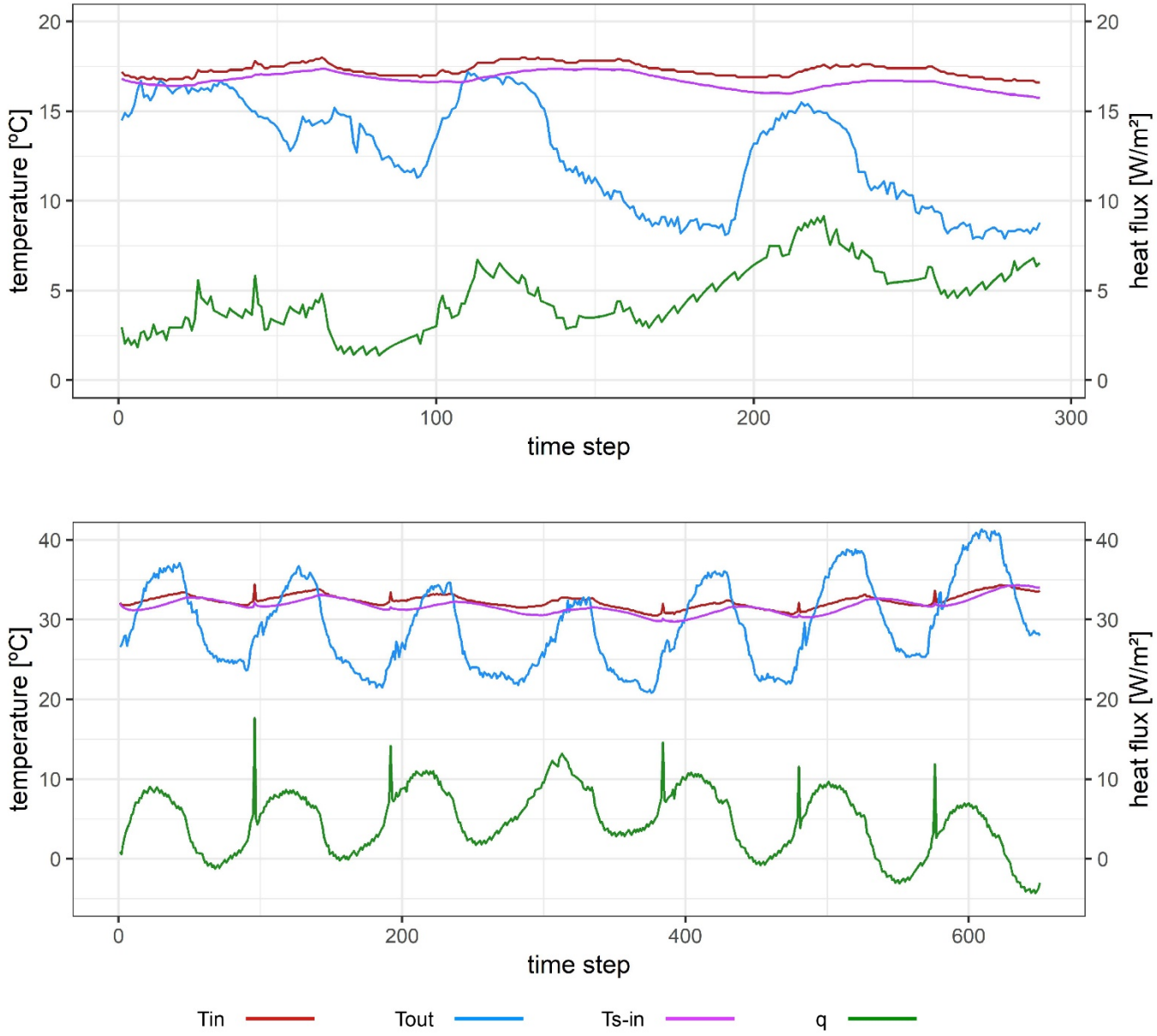

Figure 2. Example of two of the tests simulated. The former is a simulation performed under winter conditions, and the latter under summer conditions.

From the dataset, two different datasets were generated according to the output variable estimating the model: the thermal transmittance obtained with the average method, and the thermal transmittance obtained with the average method with correction for storage effect (for further information on calculation processes, see Section 2.1). Each dataset was randomly divided into two subsets: 75% of the observations corresponded to the training dataset (17,115 observations) and 25% to the testing dataset (5,705).

The testing dataset was used to determine the error of generalization of the MLPs obtained in the training phase. The performance of the estimations carried out by the MLPs were analysed by using three quality statistical parameter: the coefficient of determination (R^2) (Eq. 8), the mean absolute error (MAE) (Eq. 9), and the root mean square error ($RMSE$) (Eq. 10). Also, a total of 12 tests were selected to be individually analysed (see Table 2). Such tests were not included in the testing dataset. In addition, the same typologies of walls were not included in the training and testing datasets either (i.e., such typologies are not included in the 22,820 simulations) because the aim was to estimate in detail the thermal transmittance carried out by the models. Figure 3 sums up the flowchart followed in this research.

$$R^2 = \left(1 - \frac{\sum_{i=1}^{n} (a_i - e_i)^2}{\sum_{i=1}^{n} (a_i - \overline{a}_i)^2} \right) \tag{8}$$

$$MAE = \frac{\sum_{i=1}^{n} |a_i - e_i|}{n} \tag{9}$$

$$RMSE = \left(\frac{\sum_{i=1}^{n} (a_i - e_i)^2}{n} \right)^{1/2} \tag{10}$$

Where e_i is the estimated thermal transmittance, a_i is the actual thermal transmittance, and n is the number of observations in the dataset.

Table 2. Case studies considered for their individual analysis and the thermal transmittance results by both approaches of ISO 9869-1.

Wall	Period	U_{9869-1} [W/(m^{2}K)]	$U_{9869-1,Fk}$ [W/(m^{2}K)]
Wall P1-1	P1	1.205	1.157
Wall P1-2	P1	1.134	1.262
Wall P1-3	P1	1.475	1.422
Wall P1-4	P1	1.494	1.591
Wall P2-1	P2	1.204	1.149
Wall P2-2	P2	0.867	0.827
Wall P2-3	P2	0.715	0.764
Wall P2-4	P2	0.935	0.979
Wall P3-1	P3	0.632	0.684
Wall P3-2	P3	0.483	0.534
Wall P3-3	P3	0.613	0.691
Wall P3-4	P3	0.528	0.583

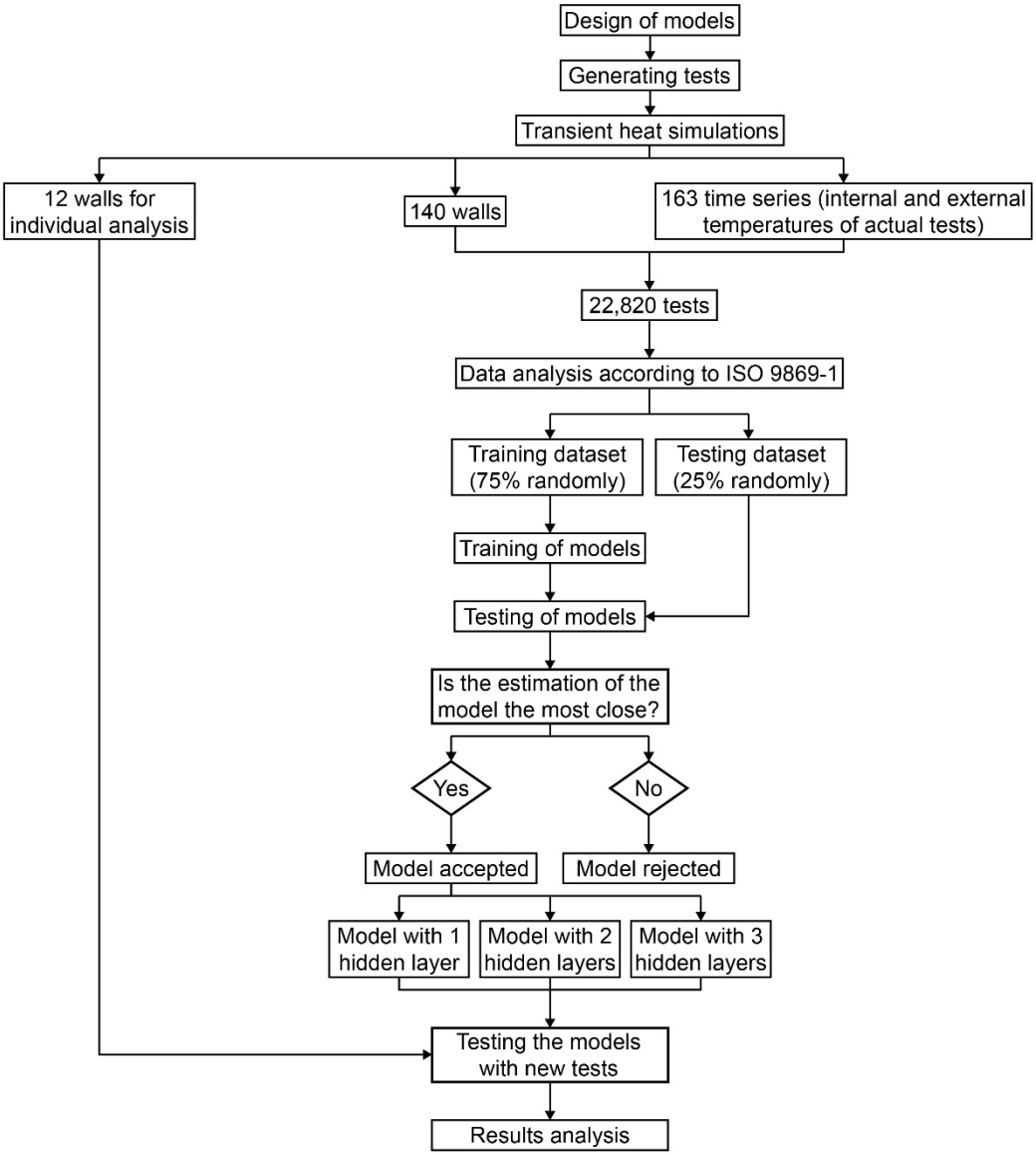

Figure 3. Flowchart of this research.

3. Results and discussion

Firstly, the performance of the MLPs was analysed to conduct estimations of the thermal transmittance obtained by approach 1 (i.e., the average method of ISO 9869-1). The most adequate architectures for MLPs of 1, 2, and 3 hidden layers were determined for this purpose. Table 3 indicates the most acceptable architectures obtained. As can be seen, the three models of MLPs presented optimal architectures with similar number of nodes: 11 for MLP_{HL-1}, 10x2 for MLP_{HL-2}, and 10x3x2 for MLP_{HL-3}. Regarding the performance obtained by the models, the degree of adjustment obtained was quite high. In this way, R^2 was in the three MLPs greater than 98.05%, and the parameters of errors (MAE and $RMSE$) obtained values lower than 0.0788 and 0.1209, respectively. Also, the capacity of generalization of the three models analysed in new instances was high. The performance obtained in the testing presented a determination coefficient oscillating between 98.30% and 99.19%, whereas MAE and $RMSE$ oscillated between 0.0437 and 0.0987, and 0.0804 and 0.1447, respectively, thus leading to a high degree of adjustment between the actual and estimated values of the testing dataset (Figure 4). Despite such high performance obtained by the three models, the architecture used in the model (i.e., the number of hidden layers) allowed the degree of adjustment obtained in new instances to be optimized. Table 3 and Figure 4 show that architectures of 2 and 3 layers obtained a more degree of adjustment: R^2 had a percentage increase oscillating between 0.52% and 0.91% with respect to the architecture of 1 layer, whereas MAE and $RMSE$ had percentage decreases greater than 54.51% and 33.52%, respectively. Such aspect was reflected in the estimated value of thermal transmittance in the walls considered for their individual analysis. As seen in Table 4, the estimations conducted by the MLP presented values close to the value obtained by the average method. Also, the percentage deviation between the actual and the estimated value was lower than 10% in most cases and MLPs analysed. Only in the estimations conducted by MLP_{HL-1} in Wall P1-1 and Wall P3-2, and by MLP_{HL-2} in Wall P3-3 had deviations slightly greater than 10%. It was also found that the estimation by the MLPs in such tests was more adjusted as the architecture had more hidden layers because of the percentage deviation average varied

from 6.24% in MLP_{HL-1} to 0.45% in MLP_{HL-3}. Moreover, there were some tests were the estimation conducted by MLP_{HL-3} was identical to the value of ISO 9869-1 (Wall P1-1, Wall P2-3, and Wall P3-2).

Table 3. Statistical parameters obtained by the MLPs estimating the thermal transmittance obtained by the average method of ISO 9869-1 (approach 1).

Model	Architecture	Training phase			Testing phase		
		R^2	MAE	$RMSE$	R^2	MAE	$RMSE$
MLP_{HL-1}	11	0.9805	0.0788	0.1209	0.9830	0.0987	0.1447
MLP_{HL-2}	10x2	0.9908	0.0507	0.0831	0.9919	0.0437	0.0804
MLP_{HL-3}	10x3x2	0.9908	0.0457	0.0821	0.9881	0.0449	0.0962

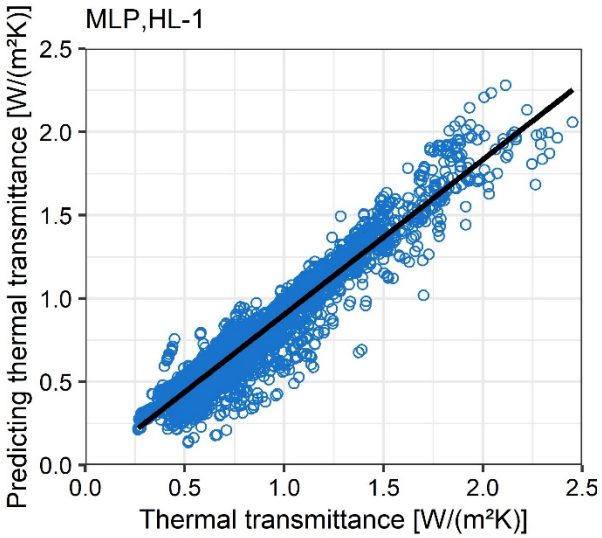

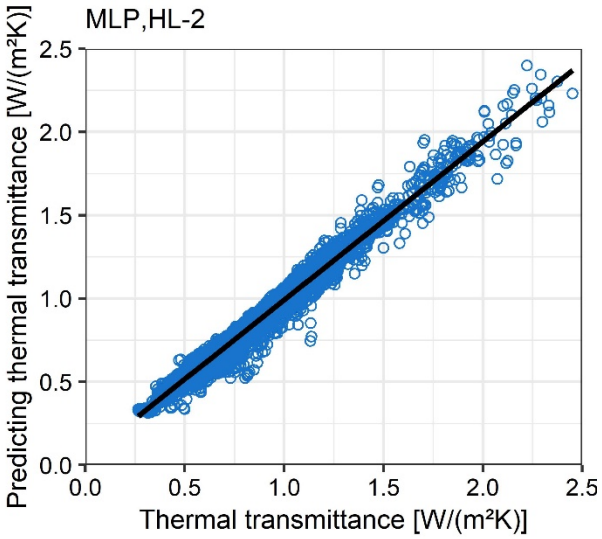

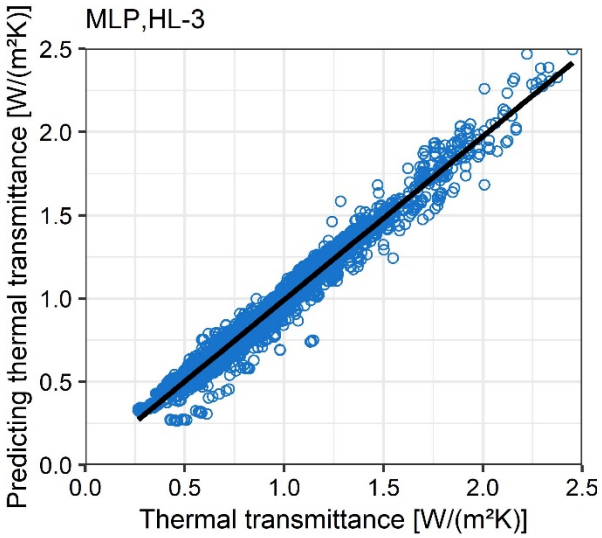

Figure 4. Point clouds between the actual and predicting thermal transmittance obtained by the average method of ISO 9869-1 (testing phase).

Table 4. Results of the estimations of thermal transmittance conducted individually in the walls analysed.

Wall	Thermal transmittance [W/(m²K)]							
	U_{9869-1}	$U_{MLP,\ 9869-1}$			$U_{9869-1,Fk}$	$U_{MLP,9869-1,Fk}$		
		MLP_{HL-1}	MLP_{HL-2}	MLP_{HL-3}		MLP_{HL-1}	MLP_{HL-2}	MLP_{HL-3}
Wall P1-1	1.205	1.075	1.146	1.209	1.157	1.193	1.089	1.180
Wall P1-2	1.134	1.054	1.111	1.155	1.262	1.197	1.131	1.092
Wall P1-3	1.475	1.390	1.412	1.439	1.422	1.345	1.336	1.374
Wall P1-4	1.494	1.486	1.453	1.432	1.591	1.516	1.533	1.528
Wall P2-1	1.204	1.199	1.267	1.239	1.149	1.222	1.125	1.136
Wall P2-2	0.867	0.786	0.891	0.856	0.827	0.784	0.790	0.791
Wall P2-3	0.715	0.703	0.734	0.720	0.764	0.739	0.736	0.799
Wall P2-4	0.935	0.881	0.976	0.932	0.979	0.968	0.953	0.994
Wall P3-1	0.632	0.579	0.666	0.647	0.684	0.719	0.634	0.682
Wall P3-2	0.483	0.414	0.465	0.483	0.534	0.520	0.495	0.534
Wall P3-3	0.613	0.586	0.686	0.659	0.691	0.639	0.611	0.672
Wall P3-4	0.528	0.494	0.498	0.517	0.583	0.582	0.540	0.576

An analysis was also performed to estimate the thermal transmittance obtained by using the MLPs of approach 2 (i.e. by the average method with correction for storage effect of ISO 9869-1). Table 5 indicates the performances obtained by the models trained in training and testing phases. Figure 5 represents the point clouds between the real and estimated values in all the tests analysed in the testing dataset. By analysing the performances obtained, it can be seen that the degree of adjustment in the training phase with the output variable was quite high: the determination coefficient oscillated between 97.30 and 98.28%, whereas MAE and $RMSE$ had low values. The degree of adjustment obtained with new data was very satisfactory. In this sense, R^2 had values greater than 98.31% and parameters of error lower than 0.0795 and 0.1254. Regarding the architecture with the best performance, the three models had similar levels of generalization. After analysing the statistical parameters obtained in the testing phase, a slight better performance in MLP_{HL-3} was found: R^2 had a percentage increase greater than 0.09% and the parameters of error had percentage decreases greater than 6.84%, thereby generating that the point clouds between the actual and estimated values were more adjusted in MLP_{HL-3}. However, the estimations conducted in the 12 tests considered for their individual analysis reflected that the deviation was not lower as the number of layers increased (Table 4). There were tests in the three MLPs in which the lowest deviation was obtained (e.g., MLP_{HL-1} obtained the lowest deviation in Wall P2-1, MLP_{HL-2} in Wall P1-1, and MLP_{HL-3} in Wall P2-2).

A different behaviour was therefore found between the models estimating $U_{MLP,\ 9869-1}$ and those estimating $U_{MLP,9869-1,Fk}$. The increase of the number of hidden layers allowed the adjustment in the output values to be optimized for the MLPs estimating the thermal transmittance obtained by the average method of ISO 9869-1, whereas the number of layers did not strongly influence their performance for models estimating the thermal transmittance with correction for storage effect. Also, the number of optimal nodes in the architectures of both typologies of MLPs were quite similar (for $U_{MLP,\ 9869-1}$, the optimal number of nodes were 11, 10x2, and 10x3x2, whereas for $U_{MLP,9869-1,Fk}$, the optimal numbers were 12, 10x4, and 10x4x2). It is worth noting that the optimization of the input variables in the MLPs improved the performances obtained with respect to that obtained in the previous work [62]. In this way, the use of the average values obtained at the end of the tests increased the determination coefficient in new instances from the 95.70% obtained in the previous study to 98.30%, thus increasing the accuracy of the values. Moreover, the total number of tests used as training and testing datasets in this paper was 22,820, instead of 69 (i.e., the number of tests increased by 329.72%). Given the degree of adjustment obtained in all tests was high because of the optimization of the MLPs, the reliability of this methodology was guaranteed.

Table 5. Statistical parameters obtained by the MLPs estimating the thermal transmittance obtained by the average method with correction for storage effect of ISO 9869-1 (approach 2).

Model	Architecture	Training phase			Testing phase		
		R^2	MAE	$RMSE$	R^2	MAE	$RMSE$
MLP_{HL-1}	12	0.9730	0.1082	0.1496	0.9831	0.0767	0.1254
MLP_{HL-2}	10x4	0.9810	0.0833	0.1241	0.9837	0.0795	0.1243
MLP_{HL-3}	10x4x2	0.9828	0.0724	0.1189	0.9846	0.0680	0.1158

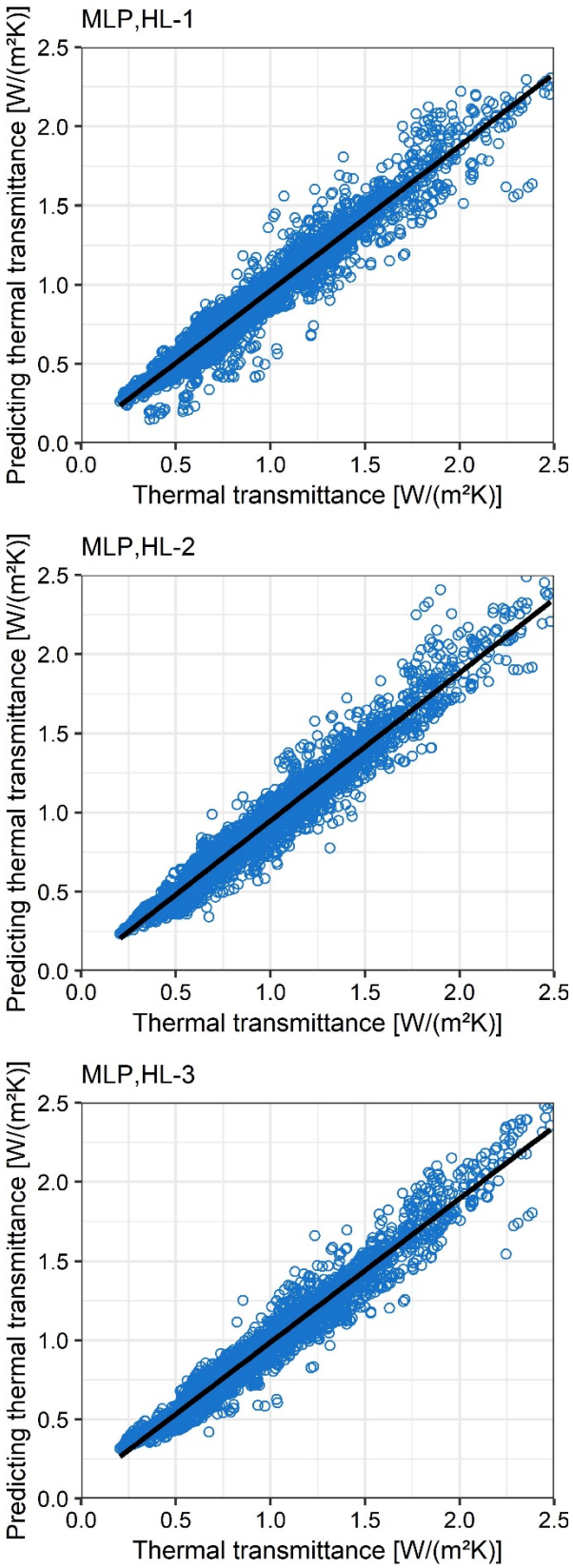

Figure 5. Point clouds between the actual and predicting thermal transmittance obtained by the average method with correction for storage effect of ISO 9869-1 (testing phase).

After analysing the performance of the MLPs, the influence of the input variables on the adjustment of the estimations was analysed. For this purpose, the existing error in the estimations conducted in the testing dataset was evaluated when the values of the different input variables were unknown. This was done by modifying the testing dataset by removing the information of the different input variables separately. Figure 6 represents the increase of MAE because of not knowing the different input variables. The effect of not knowing some of the input variables was different, although all of them generated an increase of MAE. The variables obtaining the highest incidence in the error of the estimations were $\overline{T}_{IN}$, $\overline{T}_{OUT}$, and $\overline{T}_{S-IN}$ (with increases of MAE ranging from 0.81 and 20.77 W/(m^{2}K)). This makes sense because such variables are the most directly related to the monitoring of a wall. The other two input variables related to the monitored temperatures ($\overline{\delta T}_{IN}$ and $\overline{\delta T}_{OUT}$) also influenced the performance of the models, although less than the other temperature variables. Apart from the expected influence of the temperature variables, not knowing the building period increased the error in the estimations of thermal transmittance. According to this aspect, MAE had increases oscillating between 0.39 and 0.83 W/(m^{2}K) in the testing dataset without knowing the building period. By analysing the estimations conducted in the walls for individual analysis, it was found that the error was high when the building period was unknown (Table 6). Although there were cases in which adjusted results were obtained, the percentage of representative results in the walls analysed went from 100% when knowing the building period to 16.67% without knowing the building period. Furthermore, the error in the estimations reached maximum values of 1.893 W/(m^{2}K), with average values of error greater than 0.18 W/(m^{2}K).

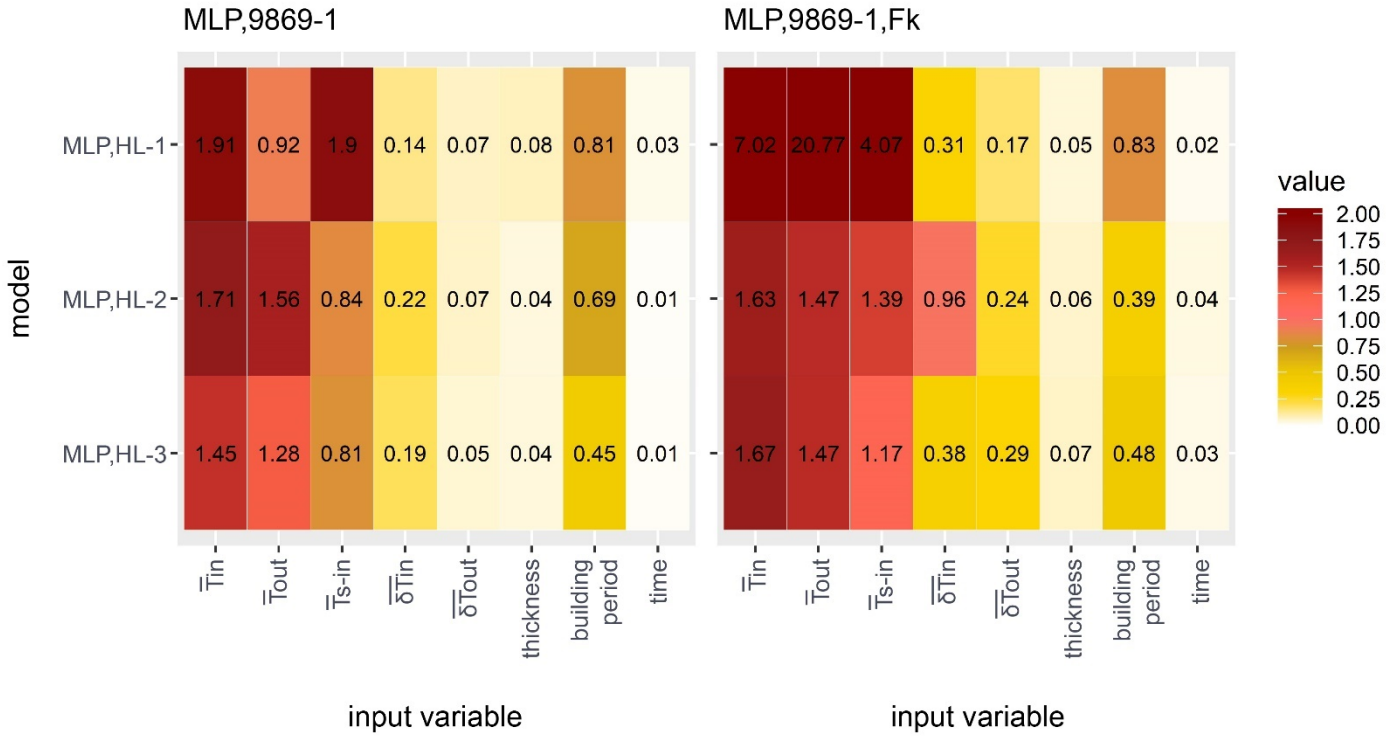

Figure 6. Heat graph with increase of MAE in the testing phase when the input variables were removed.

Table 6. Results of the estimations of thermal transmittance conducted in the walls individually analysed when their building period was unknown.

Wall	Thermal transmittance [W/(m^{2}K)]							
	U_{9869-1}	$U_{MLP,\ 9869-1}$			$U_{9869-1,Fk}$	$U_{MLP,9869-1,Fk}$		
		MLP_{HL-1}	MLP_{HL-2}	MLP_{HL-3}		MLP_{HL-1}	MLP_{HL-2}	MLP_{HL-3}
Wall P1-1	1.205	0.272	2.448	2.160	1.157	1.229	1.616	0.678
Wall P1-2	1.134	0.085	0.720	0.812	1.262	0.222	1.124	0.756
Wall P1-3	1.475	1.444	1.278	1.265	1.422	0.321	1.318	0.896
Wall P1-4	1.494	0.998	1.585	1.125	1.591	1.364	1.252	0.987
Wall P2-1	1.204	0.594	1.157	0.789	1.149	0.071	1.140	0.791
Wall P2-2	0.867	2.564	2.648	1.730	0.827	0.842	1.335	1.060
Wall P2-3	0.715	0.299	0.452	0.416	0.764	0.343	0.666	0.347
Wall P2-4	0.935	0.526	0.602	0.567	0.979	0.640	0.898	0.487
Wall P3-1	0.632	0.227	0.419	0.375	0.684	0.710	0.584	0.375
Wall P3-2	0.483	2.376	0.524	0.305	0.534	0.935	0.433	0.275
Wall P3-3	0.613	0.929	2.437	0.614	0.691	0.597	0.797	0.368

Wall P3-4	0.528	2.099	0.542	0.298	0.583	0.872	0.464	0.306

The influence of the variable of the building period on the performance of the models was therefore high. However, it can be easily determined with the consultation of cadastral data of the building, so using the MLPs is not limited. However, because of its influence on the performance of the models, the possibility of analysing the performance of individual models developed for each building period was considered in order to optimize the estimations carried out. The training dataset was therefore divided into three different subsets for each building period. By using each subset, new MLPs were developed as indicated in Section 2 and with the configuration of the most optimal architecture for each approach (Tables 3 and 5). Firstly, the statistical parameters obtained by the models of each period were analysed, as well as the accuracy in the individual walls. Figure 7 represents the statistical parameters of the MLPs estimating the thermal transmittance obtained by the average method of ISO 9869-1, whereas Figure 8 represents the statistical parameters of the MLPs with correction for storage effect. Also, Tables 7-9 indicate the estimations in the values of the thermal transmittance of the walls individually analysed. As can be seen, the use of MLPs of each period improved the performance of the periods 2 and 3 with respect to the full model. In this sense, the determination coefficient presented percentage increases oscillating between 0.31% and 1.06%, whereas the error parameters had decreases of up to 54.78%. The estimations carried out in the walls individually analysed were adjusted and had deviations oscillating between 0 and 0.072 W/(m^{2}K) (Tables 8 and 9).

The statistical parameters were worse only in the MLPs of P1 with respect to the full model. However, this aspect did not mean that the estimations carried out by the MLPs of P1 were worse. As can be seen in Table 7, the estimations performed in the 4 walls of period 1 had a greater accuracy than that obtained in the full models (see Table 4). In this way, the percentage deviation between the reference value obtained in the test and the estimated by the MLPs was lower in the models designed for P1 than in the full model: the maximum percentage deviation in the models of P1 was 5.70%, whereas in the full model was 13.47%.

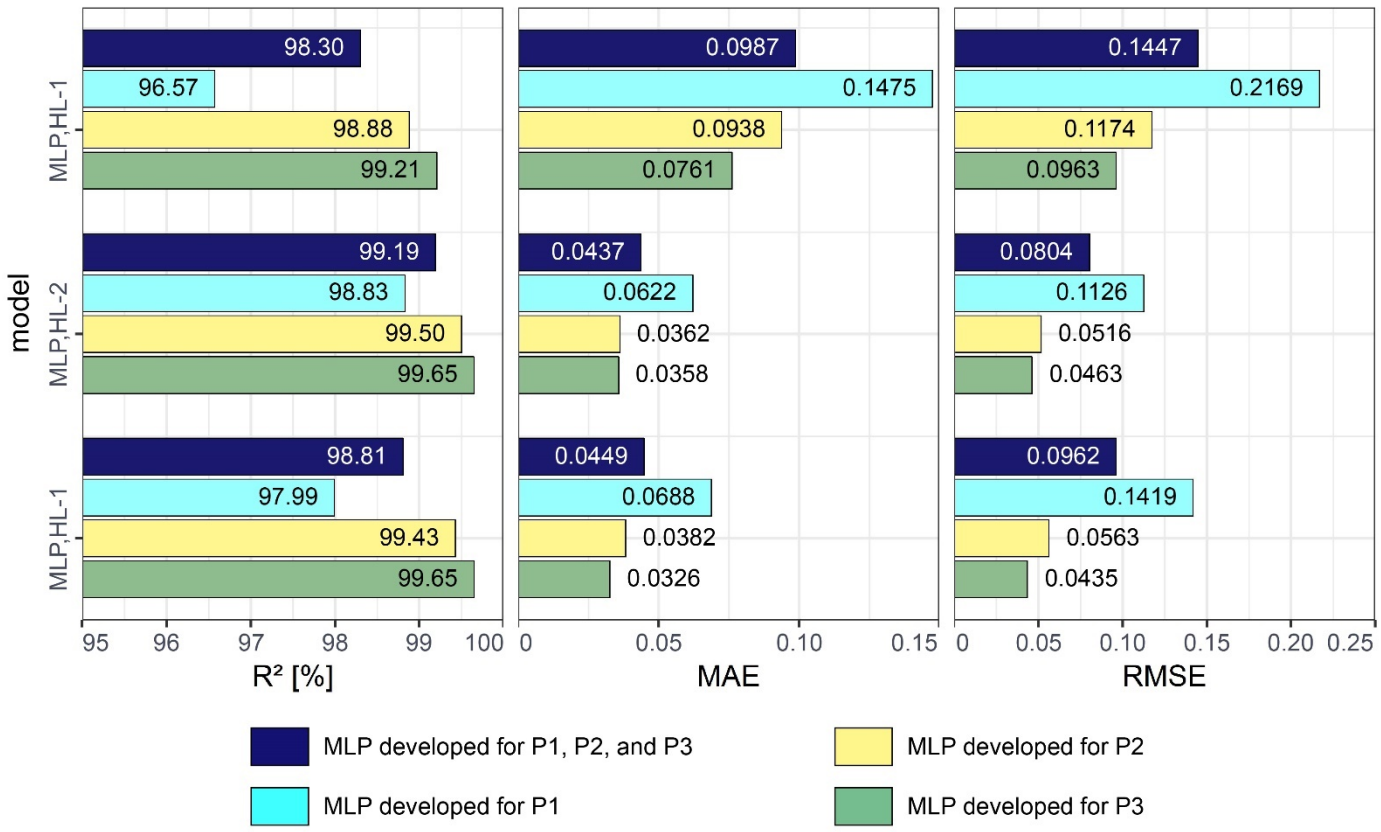

Figure 7. Comparison of the statistical parameters of the MLPs developed for each period using approach 1 (approach of the average method of ISO 9869-1).

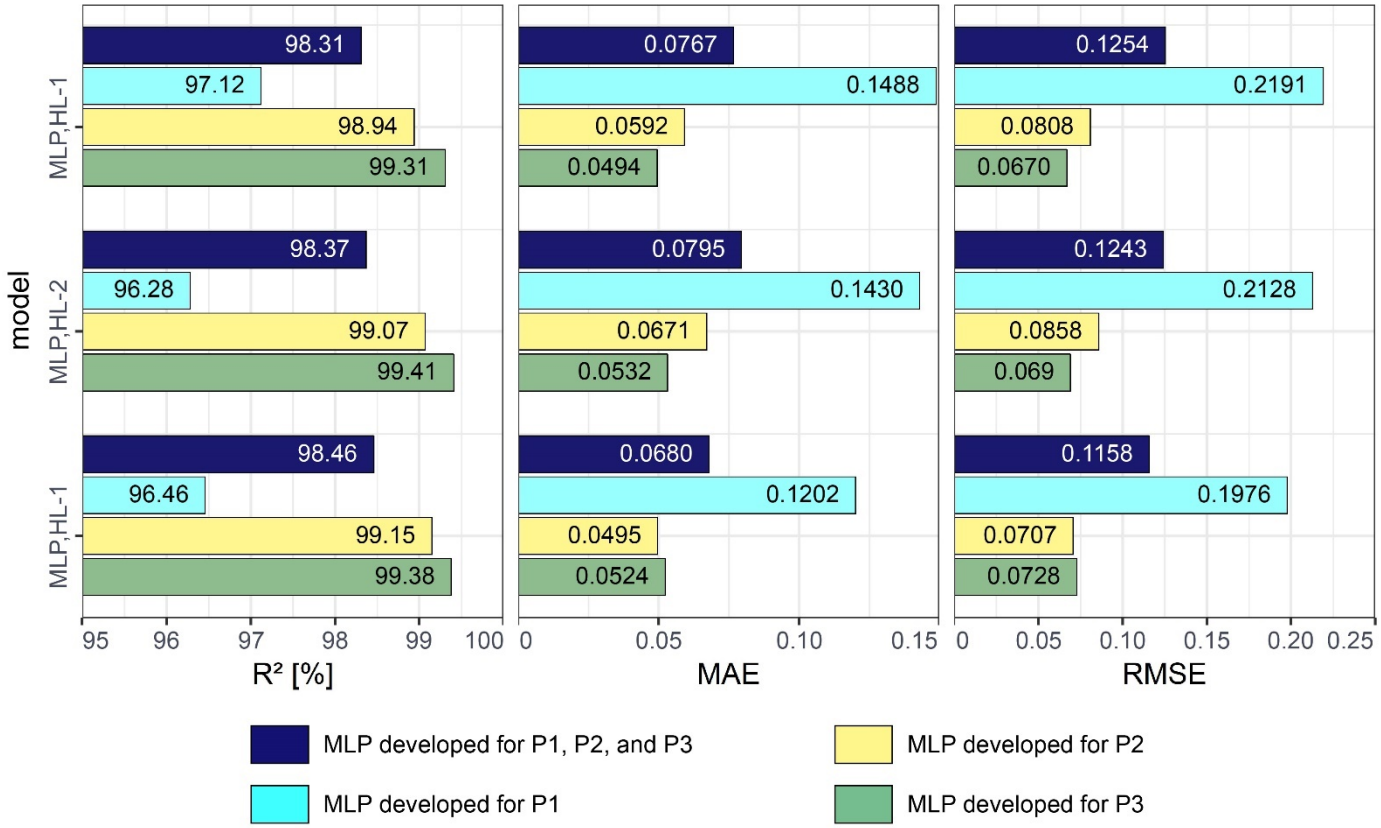

Figure 8. Comparison of the statistical parameters of the MLPs developed for each period using approach 2 (approach of the average method with correction for storage effect of ISO 9869-1).

Table 7. Results of the estimations of thermal transmittance conducted in the walls analysed by the MLPs designed for P1.

Wall	Thermal transmittance [W/(m²K)]							
	U_{9869-1}	$U_{MLP,\ 9869-1}$			$U_{9869-1,Fk}$	$U_{MLP,9869-1,Fk}$		
		MLP_{HL-1}	MLP_{HL-2}	MLP_{HL-3}		MLP_{HL-1}	MLP_{HL-2}	MLP_{HL-3}
Wall P1-1	1.205	1.145	1.165	1.189	1.157	1.096	1.125	1.091
Wall P1-2	1.134	1.143	1.086	1.212	1.262	1.250	1.282	1.183
Wall P1-3	1.475	1.463	1.452	1.508	1.422	1.351	1.428	1.477
Wall P1-4	1.494	1.426	1.472	1.537	1.591	1.539	1.517	1.509

Table 8. Results of the estimations of thermal transmittance conducted in the walls analysed by the MLPs designed for P2.

Wall	Thermal transmittance [W/(m²K)]							
	U_{9869-1}	$U_{MLP,\ 9869-1}$			$U_{9869-1,Fk}$	$U_{MLP,9869-1,Fk}$		
		MLP_{HL-1}	MLP_{HL-2}	MLP_{HL-3}		MLP_{HL-1}	MLP_{HL-2}	MLP_{HL-3}
Wall P2-1	1.204	1.180	1.260	1.172	1.149	1.102	1.126	1.191
Wall P2-2	0.867	0.839	0.907	0.852	0.827	0.884	0.797	0.843
Wall P2-3	0.715	0.676	0.770	0.707	0.764	0.799	0.694	0.782
Wall P2-4	0.935	0.881	0.983	0.934	0.979	0.994	0.907	0.945

Table 9. Results of the estimations of thermal transmittance conducted in the walls analysed by the MLPs designed for P3.

Wall	Thermal transmittance [W/(m²K)]							
	U_{9869-1}	$U_{MLP,\ 9869-1}$			$U_{9869-1,Fk}$	$U_{MLP,9869-1,Fk}$		
		MLP_{HL-1}	MLP_{HL-2}	MLP_{HL-3}		MLP_{HL-1}	MLP_{HL-2}	MLP_{HL-3}
Wall P3-1	0.632	0.614	0.606	0.611	0.684	0.682	0.724	0.660
Wall P3-2	0.483	0.488	0.482	0.503	0.534	0.534	0.506	0.484
Wall P3-3	0.613	0.649	0.623	0.603	0.691	0.672	0.731	0.700
Wall P3-4	0.528	0.573	0.582	0.530	0.583	0.576	0.537	0.589

The performance was worse for the MLPs of P1 with respect to the full model because the performance of the latter was of the 3 periods. The determination coefficient and the error parameters are therefore influenced by the best accuracy obtained in data of P2 and P3. However, the estimations carried out by the models developed for P1 were the best, as can be seen in the analysis of error of each instance composing the testing dataset. Figure 9 and 10 represent the violin plots of the errors obtained in the estimations of the testing dataset. This type of plot is an evolution of the box-plots by including information of the kernel density and rotating them to both sides of the box [87]. The density of the estimation error is therefore represented.

The use of individual models generated a decrease in the error values, as can be seen in the greatest density presented by the violin plots close to the error values equal or close to zero in most of the models analysed. In addition, the distance between the extreme values of the distribution of the errors of the individual models was lower than in full models. However, there were some cases where a better distribution of the error of the estimations of the full model was found. As for the MLPs of approach 1, for both architectures of 2 and 3 layers in P1 and for the architecture of 2 layers in P2, the estimation carried out by the full model was better than in the individual model. As for the MLPs of approach 2, the estimation of the full model was the best only in the architectures of 1 and 3 layers of P2. There was, however, a better tendency in the adjustment of the estimations of the individual models of each period with respect to the full model. The use of such models would therefore allow evaluations of thermal transmittance adjusted to different procedures of ISO 9869-1 to be performed. Also, the development of local models appropriate to the typical building periods of each region guarantees the international aspect of the results obtained.

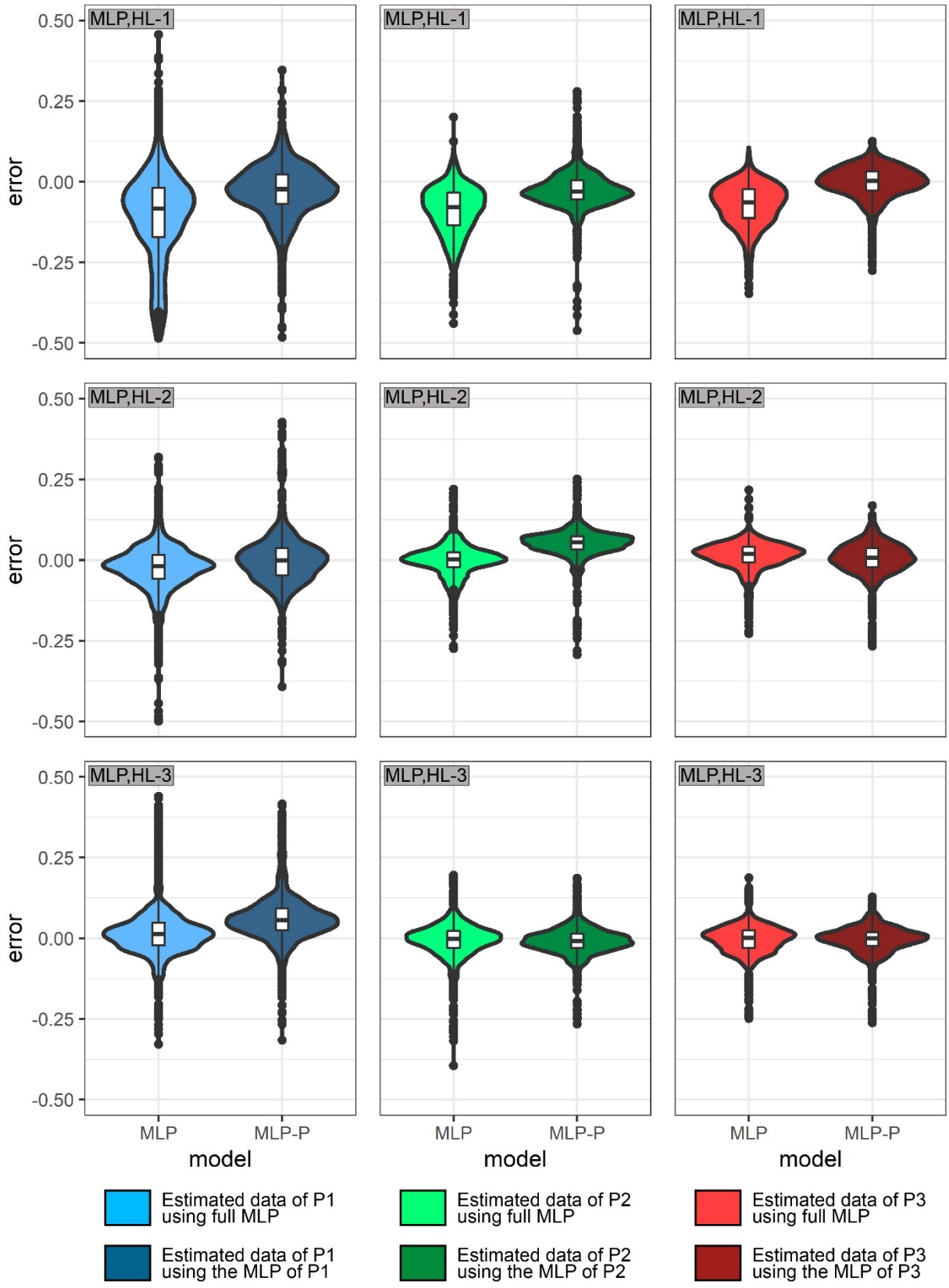

Figure 9. Violin plots with the errors obtained in the testing dataset by the various MLPs estimating the thermal transmittance obtained by the average method of ISO 9869-1 (approach 1). To make the reader's understanding easier, the box-plot of each model is represented in the violin plot. MLP identifies the models developed for all periods, and MLP-P identifies the models developed for a certain period.

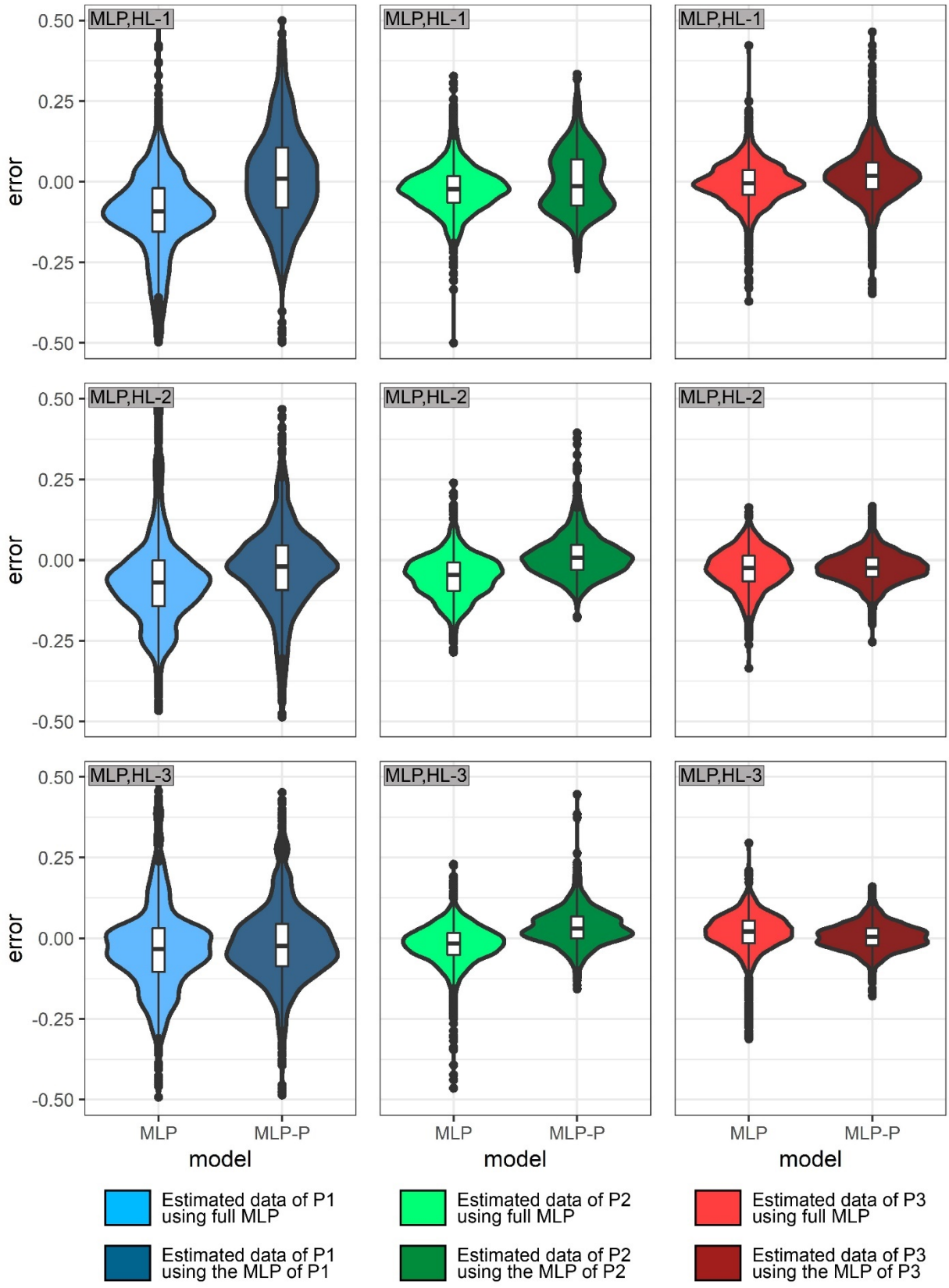

Figure 10. Violin plots with the errors obtained in the testing dataset by the various MLPs estimating the thermal transmittance obtained by the average method with correction for storage effect of ISO 9869-1 (approach 2). To make the reader's understanding easier, the box-plot of each model is represented in the violin plot. MLP identifies the models developed for all periods, and MLP-P identifies the models developed for a certain period.

4. Conclusions

The optimization in thermal characterization of walls using the thermometric method has been evaluated in this paper. For this purpose, multilayer perceptrons were used to adjust the results obtained by both approaches suggested by ISO 9869-1 to determine the thermal transmittance (the average method and the average method with correction for storage

effects). The design used for the input variables was optimized by using the design of a previous study [62]. Average variables obtained at the end of various tests were used ($\overline{T}_{IN}$, $\overline{T}_{OUT}$, $\overline{T}_{S-IN}$, $\overline{\delta T}_{IN}$, and $\overline{\delta T}_{OUT}$), as well as the test duration, and the thickness and building period of the wall, thereby simplifying their use. In addition, the variation with respect to the previous study was that the results were obtained by using the methods of ISO 9869-1, instead of those of the thermometric method. The aim was removing the possible deviations between the results obtained by both methods but maintaining the principles of the thermometric method (i.e., the measurement of the surface temperature instead of the heat flux).

Based on the results obtained of a dataset of 22,820 tests, the multilayer perceptrons carried out estimations adjusted to the values of the thermal transmittance by using the average method of ISO 9869-1. The determination coefficient was always greater than 98%. Moreover, the use of architectures of 2 and 3 hidden layers obtained more adjusted results than in architectures of 1 layer. Regarding the estimations using the correction approach of ISO 9869-1, similar results were obtained using the same number of instances (determination coefficient greater than 80%). For such approach, however, the use of more complex architectures did not improve the estimations significantly, so architectures of 1 layer can be valid. Thus, the typologies of the multilayer perceptrons designed carry out adjusted estimations of thermal transmittance obtained by the methods of ISO 9869-1, but with the variables measured by the thermometric method.

The analysis of the influence of the input variables determined that the variables resulting from the monitoring (e.g., internal and external temperature) strongly affected the accuracy of the models, whereas the thickness and the test duration had the lowest influence. The building period also had influences on the performance of the models, thus reaching average errors oscillating between 0.39 and 0.83 W/(m^{2}K). The use of the multilayer perceptrons designed particularly for each building period was therefore evaluated. The use of such new models increased the adjustment in the estimations of thermal transmittance carried out with respect to those of the full models (i.e., the models designed for all building periods). Given it is easy to determine the building period of a building (e.g., with the consultation of cadastral data), the use of individual models constitutes an opportunity to achieve more accurate results, thereby guaranteeing that the methodology is extrapolated to other regions according to their typologies and building periods. Limitations of the methodology proposed are focused on the need of having a huge and representative dataset to develop multilayer perceptrons according to each region. Their use in walls with a very low thermal transmittance (e.g., lower than 0.1 W/(m^{2}K)) is also an aspect to be analysed in future research works.

To conclude, the importance of this paper is the proposal of a methodology which allows the possible deviations in the results between the methods of ISO 9869-1 and the thermometric method to be removed. By using the results obtained by the approaches of ISO 9869-1 as output variables, the thermal transmittance can be evaluated without measuring the heat flux. In addition, the existing deviations can be avoided by using the theoretical values for the total internal heat transfer (which are not adjusted to certain types of environmental conditions and walls). More representative results with the procedures of the thermometric method can therefore be obtained by using the methodology developed in this study. Furthermore, the errors associated with the placing of the heat flux plate are removed, and a larger number of architects, engineers, and energy auditors can be guaranteed to characterize the thermal transmittance of façades correctly. A high assessment tax of the existing buildings establishing adequate energy conservation measures would be also ensured to improve the energy performance of buildings so that the goals proposed by the European Union for 2050 could be achieved.

References

[1] World Wildlife Fund, Living Planet Report 2014: Species and spaces, people and places, WWF International, Gland, Switzerland, 2014. doi:10.1007/s13398-014-0173-7.2.

[2] European Environment Agency, Final energy consumption by sector and fuel (2017), Copenhagen, Denmark, 2017. http://www.eea.europa.eu/data-and-maps/indicators/final-energy-consumption-by-sector-9/assessment-1 (accessed March 9, 2017).

[3] European Commission, Action Plan for Energy Efficiency: Realising the Potential, Brussels, Belgium, 2006.

[4] European Commission, Directive 2002/91/EC of the European Parliament and of the Council of 16 December 2002 on the energy performance of buildings, Brussels, Belgium, 2002.

[5] European Union, Directive 2010/31/EU of the European Parliament and of the Council of 19 May 2010 on the Energy Performance of Buildings, Brussels, Belgium, 2010.

[6] H. Thomson, S. Bouzarovski, C. Snell, Rethinking the measurement of energy poverty in Europe: A critical analysis of indicators and data, Indoor Built Environ. 26 (2017) 879–901. doi:10.1177/1420326X17699260.

[7] A. Pérez-Fargallo, C. Rubio-Bellido, J.A. Pulido-Arcas, M. Trebilcock, Development policy in social housing allocation: Fuel poverty potential risk index, Indoor Built Environ. 26 (2017) 980–998. doi:10.1177/1420326X17713071.

[8] C. Liddell, C. Morris, H. Thomson, C. Guiney, Excess winter deaths in 30 European countries 1980–2013: a critical review of methods, J. Public Health (Bangkok). 38 (2016) 806–814.

[9] J. Teller-Elsberg, B. Sovacool, T. Smith, E. Laine, Fuel poverty, excess winter deaths, and energy costs in Vermont: Burdensome for whom?, Energy Policy. 90 (2016). doi:10.1016/j.enpol.2015.12.009.

[10] European Commission, A Roadmap for moving to a competitive low carbon economy in 2050, Brussels, Belgium,

2011.

[11] N.A. Kurekci, Determination of optimum insulation thickness for building walls by using heating and cooling degree-day values of all Turkey's provincial centers, Energy Build. 118 (2016) 197–213. doi:10.1016/j.enbuild.2016.03.004.

[12] E.L. Vine, E. Kazakevicius, Residential energy use in Lithuania: The prospects for energy efficiency, Energy. 24 (1999) 591–603. doi:10.1016/S0360-5442(99)00013-4.

[13] A. Invidiata, M. Lavagna, E. Ghisi, Selecting design strategies using multi-criteria decision making to improve the sustainability of buildings, Build. Environ. 139 (2018) 58–68. doi:10.1016/j.buildenv.2018.04.041.

[14] C. Rubio-Bellido, A. Perez-Fargallo, J.A. Pulido-Arcas, Optimization of annual energy demand in office buildings under the influence of climate change in Chile, Energy. 114 (2016) 569–585. doi:10.1016/j.energy.2016.08.021.

[15] R. De Lieto Vollaro, C. Guattari, L. Evangelisti, G. Battista, E. Carnielo, P. Gori, Building energy performance analysis: A case study, Energy Build. 87 (2015) 87–94. doi:10.1016/j.enbuild.2014.10.080.

[16] D. Bienvenido-Huertas, J.A.F. Quiñones, J. Moyano, C.E. Rodríguez-Jiménez, Patents Analysis of Thermal Bridges in Slab Fronts and Their Effect on Energy Demand, Energies. 11 (2018) 2222. doi:10.3390/en11092222.

[17] R. Adhikari, E. Lucchi, V. Pracchi, Experimental measurements on thermal transmittance of the opaque vertical walls in the historical buildings, in: PLEA2012 Conf. Oppor. Limits Needs Towar. an Environ. Responsible Archit., 2012.

[18] W. Natephra, N. Yabuki, T. Fukuda, Optimizing the evaluation of building envelope design for thermal performance using a BIM-based overall thermal transfer value calculation, Build. Environ. 136 (2018) 128–145. doi:10.1016/j.buildenv.2018.03.032.

[19] G.K. Oral, Z. Yilmaz, The limit U values for building envelope related to building form in temperate and cold climatic zones, Build. Environ. 37 (2002) 1173–1180. doi:10.1016/S0360-1323(01)00102-0.

[20] A. Prada, F. Cappelletti, P. Baggio, A. Gasparella, On the effect of material uncertainties in envelope heat transfer simulations, Energy Build. 71 (2014) 53–60. doi:10.1016/j.enbuild.2013.11.083.

[21] D. Bienvenido-huertas, J. Moyano, D. Marín, R. Fresco-Contreras, Review of in situ methods for assessing the thermal transmittance of walls, Renew. Sustain. Energy Rev. 102 (2019) 356–371. doi:10.1016/j.rser.2018.12.016.

[22] W. Bustamante, A. Bobadilla, B. Navarrete, G. Saelzer, S. Vidal, Uso eficiente de la energía en edificios habitacionales. Mejoramiento térmico de muros de albañilería de ladrillos cerámicos. El caso de Chile, Rev. La Construcción. 4 (2005) 5–12.

[23] M. de Luxán García de Diego, G. Gómez Muñoz, E. Román López, Towards new energy accounting in residential building, Inf. La Construcción. 67 (2015) 1–10. doi:10.3989/ic.14.059.

[24] N. Soares, C. Martins, M. Gonçalves, P. Santos, L.S. da Silva, J.J. Costa, Laboratory and in-situ non-destructive methods to evaluate the thermal transmittance and behavior of walls, windows, and construction elements with innovative materials: A review, Energy Build. 182 (2019) 88–110. doi:10.1016/j.enbuild.2018.10.021.

[25] International Organization for Standardization, ISO 6946:2007 - Building components and building elements - Thermal resistance and thermal transmittance - Calculation method, Geneva, Switzerland, 2007.

[26] G. Ficco, F. Iannetta, E. Ianniello, F.R. D'Ambrosio Alfano, M. Dell'Isola, U-value in situ measurement for energy diagnosis of existing buildings, Energy Build. 104 (2015) 108–121. doi:10.1016/j.enbuild.2015.06.071.

[27] I. Ballarini, S.P. Corgnati, V. Corrado, Use of reference buildings to assess the energy saving potentials of the residential building stock: The experience of TABULA project, Energy Policy. 68 (2014) 273–284. doi:10.1016/j.enpol.2014.01.027.

[28] L. Evangelisti, C. Guattari, P. Gori, R. De Lieto Vollaro, In situ thermal transmittance measurements for investigating differences between wall models and actual building performance, Sustainability. 7 (2015) 10388–10398. doi:10.3390/su70810388.

[29] D. Bienvenido-Huertas, R. Rodríguez-Álvaro, J.J. Moyano, F. Rico, D. Marín, Determining the U-Value of Façades Using the Thermometric Method: Potentials and Limitations, Energies. 11 (2018) 1–17. doi:10.3390/en11020360.

[30] V. Echarri, A. Espinosa, C. Rizo, Thermal transmission through existing building enclosures: Destructive monitoring in intermediate layers versus non-destructive monitoring with sensors on surfaces, Sensors. 17 (2017) 1–24. doi:10.3390/s17122848.

[31] G. Litti, S. Khoshdel, A. Audenaert, J. Braet, Hygrothermal performance evaluation of traditional brick masonry in historic buildings, Energy Build. 105 (2015) 393–411. doi:10.1016/j.enbuild.2015.07.049.

[32] D.S. Choi, M.J. Ko, Comparison of Various Analysis Methods Based on Heat Flowmeters and Infrared Thermography Measurements for the Evaluation of the In Situ Thermal Transmittance of Opaque Exterior Walls, Energies. 10 (2017) 1–22. doi:10.3390/en10071019.

[33] J.M. Pérez-Bella, J. Domínguez-Hernández, E. Cano-Suñén, J.J. Del Coz-Díaz, B.R. Soria, Adjusting the design thermal conductivity considered by the Spanish building technical code for façade materials, Dyna. 92 (2017) 1–11. doi:10.6036/8005.

[34] International Organization for Standardization, ISO 9869-1:2014 - Thermal insulation - Building elements - In situ measurement of thermal resistance and thermal transmittance. Part 1: Heat flow meter method, Geneva, Switzerland, 2014.

[35] R. Albatici, A.M. Tonelli, M. Chiogna, A comprehensive experimental approach for the validation of quantitative infrared thermography in the evaluation of building thermal transmittance, Appl. Energy. 141 (2015) 218–228. doi:10.1016/j.apenergy.2014.12.035.

[36] P.A. Fokaides, S.A. Kalogirou, Application of infrared thermography for the determination of the overall heat transfer coefficient (U-Value) in building envelopes, Appl. Energy. 88 (2011) 4358–4365. doi:10.1016/j.apenergy.2011.05.014.

[37] S.-H. Kim, J.-H. Kim, H.-G. Jeong, K.-D. Song, Reliability Field Test of the Air–Surface Temperature Ratio Method for In Situ Measurement of U-Values, Energies. 11 (2018) 1–15. doi:10.3390/en11040803.

[38] S.-H. Kim, J.-H. Lee, J.-H. Kim, S.-H. Yoo, H.-G. Jeong, The Feasibility of Improving the Accuracy of In Situ Measurements in the Air-Surface Temperature Ratio Method, Energies. 11 (2018) 1–18. doi:10.3390/en11071885.

[39] C. Peng, Z. Wu, In situ measuring and evaluating the thermal resistance of building construction, Energy Build. 40 (2008) 2076–2082. doi:10.1016/j.enbuild.2008.05.012.

[40] H. Trethowen, Measurement errors with surface-mounted heat flux sensors, Build. Environ. 21 (1986) 41–56. doi:10.1016/0360-1323(86)90007-7.

[41] G. Desogus, S. Mura, R. Ricciu, Comparing different approaches to in situ measurement of building components thermal resistance, Energy Build. 43 (2011) 2613–2620. doi:10.1016/j.enbuild.2011.05.025.

[42] P.G. Cesaratto, M. De Carli, S. Marinetti, Effect of different parameters on the in situ thermal conductance evaluation, Energy Build. 43 (2011) 1792–1801. doi:10.1016/j.enbuild.2011.03.021.

[43] M. Cucumo, A. De Rosa, V. Ferraro, D. Kaliakatsos, V. Marinelli, A method for the experimental evaluation in situ of the wall conductance, Energy Build. 38 (2006) 238–244. doi:10.1016/j.enbuild.2005.06.005.

[44] X. Meng, B. Yan, Y. Gao, J. Wang, W. Zhang, E. Long, Factors affecting the in situ measurement accuracy of the wall heat transfer coefficient using the heat flow meter method, Energy Build. 86 (2015) 754–765. doi:10.1016/j.enbuild.2014.11.005.

[45] L. Evangelisti, C. Guattari, F. Asdrubali, Influence of heating systems on thermal transmittance evaluations: Simulations, experimental measurements and data post-processing, Energy Build. 168 (2018) 180–190. doi:10.1016/j.enbuild.2018.03.032.

[46] F. Björk, T. Enochsson, Properties of thermal insulation materials during extreme environment changes, Constr. Build. Mater. 23 (2009) 2189–2195. doi:10.1016/j.conbuildmat.2008.12.006.

[47] C. Guattari, L. Evangelisti, P. Gori, F. Asdrubali, Influence of internal heat sources on thermal resistance evaluation through the heat flow meter method, Energy Build. 135 (2017) 187–200. doi:10.1016/j.enbuild.2016.11.045.

[48] A. Ahmad, M. Maslehuddin, L.M. Al-Hadhrami, In situ measurement of thermal transmittance and thermal resistance of hollow reinforced precast concrete walls, Energy Build. 84 (2014) 132–141. doi:10.1016/j.enbuild.2014.07.048.

[49] K. Gaspar, M. Casals, M. Gangolells, Review of criteria for determining HFM minimum test duration, Energy Build. 176 (2018) 360–370. doi:10.1016/j.enbuild.2018.07.049.

[50] E. Lucchi, Thermal transmittance of historical brick masonries: A comparison among standard data, analytical calculation procedures, and in situ heat flow meter measurements, Energy Build. 134 (2017) 171–184. doi:10.1016/j.enbuild.2016.10.045.

[51] E. Lucchi, Thermal transmittance of historical stone masonries: A comparison among standard, calculated and measured data, Energy Build. 151 (2017) 393–405. doi:10.1016/j.enbuild.2017.07.002.

[52] M. Rotilio, F. Cucchiella, P. De Berardinis, V. Stornelli, Thermal Transmittance Measurements of the Historical Masonries: Some Case Studies, Energies. 11 (2018) 2987. doi:10.3390/en11112987.

[53] K. Gaspar, M. Casals, M. Gangolells, Energy & Buildings In situ measurement of façades with a low U-value : Avoiding deviations, Energy Build. 170 (2018) 61–73. doi:10.1016/j.enbuild.2018.04.012.

[54] F. Asdrubali, F. D'Alessandro, G. Baldinelli, F. Bianchi, Evaluating in situ thermal transmittance of green buildings masonries: A case study, Case Stud. Constr. Mater. 1 (2014) 53–59. doi:10.1016/j.cscm.2014.04.004.

[55] I. Nardi, E. Lucchi, T. de Rubeis, D. Ambrosini, Quantification of heat energy losses through the building envelope: A state-of-the-art analysis with critical and comprehensive review on infrared thermography, Build. Environ. 146

(2018) 190–205. doi:10.1016/j.buildenv.2018.09.050.

[56] D. Bienvenido-Huertas, J. Bermúdez, J. Moyano, D. Marín, Comparison of quantitative IRT to estimate U-value using different approximations of ECHTC in multi-leaf walls, Energy Build. 184 (2018) 99–113. doi:10.1016/j.enbuild.2018.11.028.

[57] D. Bienvenido-Huertas, J. Bermúdez, J.J. Moyano, D. Marín, Influence of ICHTC correlations on the thermal characterization of façades using the quantitative internal infrared thermography method, Build. Environ. 149 (2019) 512–525. doi:10.1016/j.buildenv.2018.12.056.

[58] R. Albatici, A.M. Tonelli, Infrared thermovision technique for the assessment of thermal transmittance value of opaque building elements on site, Energy Build. 42 (2010) 2177–2183. doi:10.1016/j.enbuild.2010.07.010.

[59] B. Tejedor, M. Casals, M. Gangolells, Assessing the influence of operating conditions and thermophysical properties on the accuracy of in-situ measured U-values using quantitative internal infrared thermography, Energy Build. 171 (2018) 64–75. doi:10.1016/j.enbuild.2018.04.011.

[60] B. Tejedor, M. Casals, M. Gangolells, X. Roca, Quantitative internal infrared thermography for determining in-situ thermal behaviour of façades, Energy Build. 151 (2017) 187–197. doi:10.1016/j.enbuild.2017.06.040.

[61] J.M. Andújar Márquez, M.Á. Martínez Bohórquez, S. Gómez Melgar, A new metre for cheap, quick, reliable and simple thermal transmittance (U-Value) measurements in buildings, Sensors. 17 (2017) 1–18. doi:10.3390/s17092017.

[62] D. Bienvenido-Huertas, J. Moyano, C.E. Rodríguez-Jiménez, D. Marín, Applying an artificial neural network to assess thermal transmittance in walls by means of the thermometric method, Appl. Energy. 233–234 (2019) 1–14. doi:10.1016/j.apenergy.2018.10.052.

[63] L. Evangelisti, C. Guattari, P. Gori, R. de Lieto Vollaro, F. Asdrubali, Experimental investigation of the influence of convective and radiative heat transfers on thermal transmittance measurements, Int. Commun. Heat Mass Transf. 78 (2016) 214–223. doi:10.1016/j.icheatmasstransfer.2016.09.008.

[64] C. Buratti, L. Barelli, E. Moretti, Application of artificial neural network to predict thermal transmittance of wooden windows, Appl. Energy. 98 (2012) 425–432. doi:10.1016/j.apenergy.2012.04.004.

[65] S. Chudzik, Applying infrared measurements in a measuring system for determining thermal parameters of thermal insulation materials, Infrared Phys. Technol. 81 (2017) 296–304. doi:10.1016/j.infrared.2016.12.025.

[66] F. Aznar, V. Echarri, C. Rizo, R. Rizo, Modelling the thermal behaviour of a building facade using deep learning, PLoS One. 13 (2018) 1–20. doi:10.1371/journal.pone.0207616.

[67] A.H. Deconinck, S. Roels, Comparison of characterisation methods determining the thermal resistance of building components from onsite measurements, Energy Build. 130 (2016) 309–320. doi:10.1016/j.enbuild.2016.08.061.

[68] A.R. Barron, Universal approximation bounds for superpositions of a sigmoidal function, IEEE Trans. Inf. Theory. 39 (1993) 930–945.

[69] G. Cybenko, Approximation by superpositions of a sigmoidal function, Math. Control. Signals Syst. 2 (1989) 303–314.

[70] K. Hornik, M. Stinchcombe, H. White, Multilayer feedforward networks are universal approximators, Neural Networks. 2 (1989) 359–366. doi:10.1016/0893-6080(89)90020-8.

[71] S.S. Haykin, S.S. Haykin, S.S. Haykin, S.S. Haykin, Neural networks and learning machines, Pearson Upper Saddle River, 2009.

[72] D. Bienvenido-Huertas, C. Rubio-Bellido, J. Pérez-Ordóñez, F. Martínez-Abella, Estimating Adaptive Setpoint Temperatures Using Weather Stations, Energies. 12 (2019) 1197. doi:10.3390/en12071197.

[73] S. Raghu, N. Sriraam, Optimal configuration of multilayer perceptron neural network classifier for recognition of intracranial epileptic seizures, Expert Syst. Appl. 89 (2017) 205–221. doi:10.1016/j.eswa.2017.07.029.

[74] M. Gangolells, M. Casals, N. Forcada, M. MacArulla, E. Cuerva, Energy mapping of existing building stock in Spain, J. Clean. Prod. 112 (2016) 3895–3904. doi:10.1016/j.jclepro.2015.05.105.

[75] K. Gaspar, M. Casals, M. Gangolells, Classifying system for façades and anomalies, J. Perform. Constr. Facil. 30 (2014) 4014187.

[76] The Government of Spain, Royal Decree 2429/79. Approving the Basic Building Norm NBE-CT-79, about the Thermal Conditions in Buildings, 1979.

[77] The Government of Spain, Royal Decree 314/2006. Approving the Spanish Technical Building Code, Madrid, Spain, 2013.

[78] F. Kurtz, M. Monzón, B. López-Mesa, Energy and acoustics related obsolescence of social housing of Spain's post-war in less favoured urban areas. The case of Zaragoza, Inf. La Construcción. 67 (2015) m021. doi:10.3989/ic.14.062.

[79] V.F. Membrive, L.B. Xavier, F.P. Isabel, Clasificación energética de edificios. Efectos del cambio en la normativa y los

métodos constructivos en la zona climática española A4, Obs. Medioambient. 16 (2013) 69–98.

[80] D.E. Rumelhart, G.E. Hinton, R.J. Williams, Learning representations by back-propagating errors, Nature. 323 (1986) 533–536. doi:10.1038/323533a0.

[81] Y.N. Wang, A neural network adaptive control based on rapid learning method and application, Adv. Molding Anal. 46 (1994) 27–34.

[82] P. Werbos, Beyond Regression: New Tools for Prediction and Analysis in the Behavior Science, Harvard University, 1974.

[83] R. Fletcher, Practical methods of optimization, John Wiley&Sons, Chichester - New York - Brisbane - Toronto, United States, 1980.

[84] R. Kohavi, A Study of Cross-Validation and Bootstrap for Accuracy Estimation and Model Selection, in: Int. Jt. Conf. Artif. Intell., 1995. doi:10.1067/mod.2000.109031.

[85] Eduardo Torroja Institute for Construction Science, Constructive elements catalogue of the CTE, 2010.

[86] S. Domínguez-Amarillo, J.J. Sendra, I. Oteiza, La envolvente térmica de la vivienda social. El caso de Sevilla, 1939 a 1979, Editorial CSIC: Madrid, 2016.

[87] J.L. Hintze, R.D. Nelson, Violin Plots: A Box Plot-Density Trace Synergism, Am. Stat. 52 (1998) 181–184. doi:10.1080/00031305.1998.10480559.